Energy Storage Materials 38 (2021) 30–49

Contents lists available at ScienceDirect

Energy Storage Materials

journal homepage: www.elsevier.com/locate/ensm

Comprehensive Insights into Electrolytes and Solid Electrolyte Interfaces in Potassium-Ion Batteries

Xiao Zhang[a], Jiashen Meng[a], Xuanpeng Wang[b,c,d,*], Zhitong Xiao[a], Peijie Wu[a], Liqiang Mai[a,c,*]

[a] State Key Laboratory of Advanced Technology for Materials Synthesis and Processing, School of Materials Science and Engineering, Wuhan University of Technology, Wuhan 430070, P. R. China
[b] Department of Physical Science & Technology, School of Science, Wuhan University of Technology, Wuhan 430070, P. R. China
[c] Foshan Xianhu Laboratory of the Advanced Energy Science and Technology Guangdong Laboratory, Xianhu hydrogen Valley, Foshan 528200, P. R. China
[d] Guangzhou Key Laboratory of Clean Transportation Energy Chemistry, Guangdong University of Technology, Guangzhou 510006, P. R. China

ARTICLE INFO

Keywords:
Potassium-ion batteries
electrolytes
solid electrolyte interfaces
influence factors
interface engineering strategies

ABSTRACT

Potassium-ion batteries (KIBs) are competitive alternatives to lithium-ion batteries (LIBs) due to the abundant K resources and high energy density. As an indispensable part of the battery, the electrolyte affects the battery capacity, rate capability, cycle life, and safety. Nevertheless, the researches on electrolytes and corresponding solid electrolyte interfaces (SEI) in KIB are still in its infancy and require further attention. In this review, recent progresses of various K^+ containing electrolytes for KIBs are summarized comprehensively. Additionally, the effects of salts, solvents, additives, and concentrations on the properties of various electrolyte systems are discussed in detail. Thereafter, interface chemistry between electrode and electrolyte, as well as rational modification strategies for high-performance KIB are reviewed. Finally, the major challenges and the future perspectives are estimated for advanced KIB. This review will provide good directions for the development of high-performance KIB.

1. Introduction

Energy storage technology integrating intermittent energy has become the focus of attention with the rapid rise of renewable energy. Developing large-scale energy storage systems with high-efficiency is a key strategy to realize the application of renewable energy and the construction of national smart grids. Lithium-ion battery (LIB) as a chemical energy storage technology has been favored by the field of automotive power batteries owing to high energy density and high working voltage [1–3]. However, the raw materials of LIB, namely lithium and cobalt resources, are affected by reserves and the market [4,5]. Potassium-ion battery (KIB) and sodium-ion battery (SIB) are possible alternatives to LIB owing to the abundant content of K and Na in the earth's crust (Figure 1a) [6–15]. Moreover, the prices of potassium salt (K_2CO_3) and Na_2CO_3 as raw materials for electrodes are much cheaper than Li_2CO_3. In addition, both KIB and SIB reduce the battery costs and the weight of the current collector by using aluminum (Al) as the anode collector to replace copper required by LIB, because K and Na do not form any Al-K/Na intermetallic compounds [16]. However, KIB provides several more important advantages than SIB. First, KIB is expected to provide higher-voltage operation than NIB or even LIB. The redox potential of K/K^+ (−2.93 V vs standard hydrogen electrode (SHE)) is close to Li/Li^+ (−3.04 V vs SHE), which is lower than Na/Na^+(−2.71 V vs SHE) (Figure 1b). In addition, it has been confirmed that the standard electrode potential of K is lower than that of Li/Li^+ in propylene carbonate (PC) or ethylene carbonate (EC)/diethyl carbonate (DEC), which means that KIB shows the potential to provide high voltage than LIB [10,17]. Second, KIB is expected to have higher power capability due to the rapid diffusion of K^+. Although K^+ has the largest ion radius compared to Na^+ and Li^+, it has the smallest Stokes radius in PC (Figure 1c). The weak Lewis acidity of K^+ makes the weak interaction between K^+ and solvent molecules, which in turn makes K^+ diffuse the fastest in the electrolyte solution and the molar conductivity is the highest. Moreover, the desolvation energy of K^+ in PC is much lower than that of Na^+ and Li^+, which makes KIB expected to exhibit higher rate capability than LIB and SIB (Figure 1d) [18]. However, the poor diffusion of K^+ with large ion radius in solids limits the reaction kinetics of KIB. During K^+ insertion/extraction process, the volume change of the electrode material in KIB will be more obvious than that of SIB and LIB. The lower electrochemical potential makes it easier for the solvent in the electrolyte to be reduced on the electrode surface in KIB, causing serious side reactions to occur. Compared with Na and Li, K has a lower melting point and stronger reactivity. Thus, the growth of K dendrites and battery safety are more concerned.

The number of reported scientific publications on KIB has increased exponentially in recent years (Figure 1e). Up to now, numerous

* Corresponding author.
E-mail addresses: wxp122525691@whut.edu.cn (X. Wang), mlq518@whut.edu.cn (L. Mai).

https://doi.org/10.1016/j.ensm.2021.02.036
Received 14 December 2020; Received in revised form 26 January 2021; Accepted 20 February 2021
Available online 23 February 2021

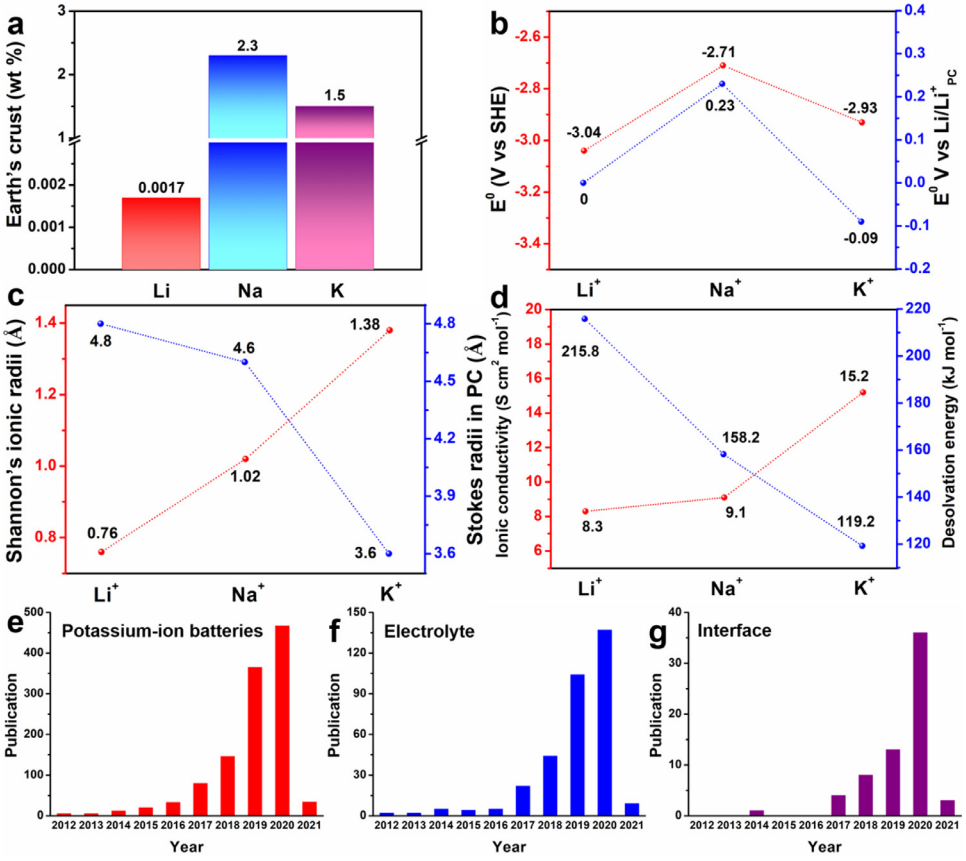

Figure 1. (a) Abundance of Li, Na, and K metal in Earth's crust (wt %). Comparison of (b) potential, (c) radius, (d) ionic conductivity and desolvation energy of Li^+, Na^+, and K^+. Number of publications dealing with (e) "Potassium-ion batteries", (f) "Potassium-ion batteries + electrolyte", and (g) "Potassium-ion batteries + electrolyte + interface" in web of science (Jan 22, 2021).

researches have been devoted to developing high-voltage cathode materials and high-capacity anode materials to realize the high energy density KIB. Nevertheless, the structure of the electrode material changes greatly during the charge and discharge processes, which in turn causes rapid capacity degradation. The existing strategies include the design of nanostructures, the recombination of carbon matrix, and the introduction of defects or vacancies by heteroatom doping, etc [11–13,19–23]. However, high-performance electrodes are inseparable from the compatible electrolyte [24,25]. In this regard, the compatible electrolytes and understanding/optimization of interfaces are getting more and more attention, which can be clearly observed in many publications (Figure 1f and g). The electrolyte affects the overall performance of the battery through interface chemistry, including battery capacity, rate capability, cycle life and safety [26,27]. As for organic electrolytes, the formulations for KIB are continuously optimized to obtain more excellent electrochemical performance. For an instance, the electrochemical window of $KClO_4$/PC solutions was studied as early as 2001 [28]. Subsequently, a KIB was designed using KBF_4-EC/ethyl methyl carbonate (EMC) electrolyte [8]. However, poor conductivity and low solubility of $KClO_4$ and KBF_4 hinder the development of corresponding electrolytes. Then, the behavior of K^+ inserting into graphite in KPF_6-EC/DEC electrolyte was reported firstly [16,29]. Recently, some researches have been devoted to the development of high-performance KIB electrolytes. They use different K salts with different organic solvents, adjust the salt concentrations, optimize the solvent ratios, or use additives to improve the interface composition, thereby improving the Coulombic efficiency (CE) and extending the battery cycle life. But they also suffer from the high cost and low safety. To address the problems in organic electrolytes, various electrolytes such as aqueous electrolyte, ionic liquid (IL) electrolyte, and solid electrolyte were proposed.

Many important scientific issues related to the complex reactions that occur at the electrode/electrolyte interface (including the reaction mechanism, the composition of the passivation film, and the modification strategy) are of great significance for improving the electrochemical performance of KIB. Especially, a stable passivation film formed in a suitable electrolyte can avoid the occurrence of side reaction and inhibit the growth of K dendrites, while the unstable solid electrolyte interface (SEI) will lead to poor electrochemical performance in incompatible electrolyte. Although great progress has been made in electrolyte design to improve the electrochemical performance of KIB, there are still several major problems summarized as follows: (1) lack of K salt options, (2) serious side reactions caused by highly active K metal, (3) the compatibility of electrolytes and electrode materials (unstable SEI), (4) lack of high-voltage-resistant electrolyte system, (5) the growth of K dendrite, (6) lack of advanced characterization techniques to better understand K^+ solvation and transport characteristics [10,30,31]. Overall, the development of high-performance KIB in the future will depend on the discovery and development of state-of-the-art electrolytes, as well as a comprehensive grasp of the interface of the electrolyte and electrode.

Herein, this review aims to provide a comprehensive overview of electrolyte design and SEI layers for high-performance KIB. First, basic chemistry, classifications, and design principles of KIB electrolytes are introduced. Then, the influence of three components (salts, solvents, and additives) and concentrations on various electrolytes is summarized and discussed. Furthermore, the SEI on various electrodes are presented, including the SEI formation mechanism, the composition of SEI films, K^+ transport manners, influencing factors of the SEI in various electrodes, and effective modification of the SEI (Figure 2). Finally, the challenges and opportunities of KIB electrolytes and SEI are analyzed and proposed.

2. KIB Electrolytes

2.1. Design Principle of KIB Electrolytes Based on Fundamental/Basic Chemistry

KIB follows a rocking-chair type working principle similar to LIB and SIB, which is based on the shuttlecock of K^+ between positive and negative electrodes during the charge and discharge processes in

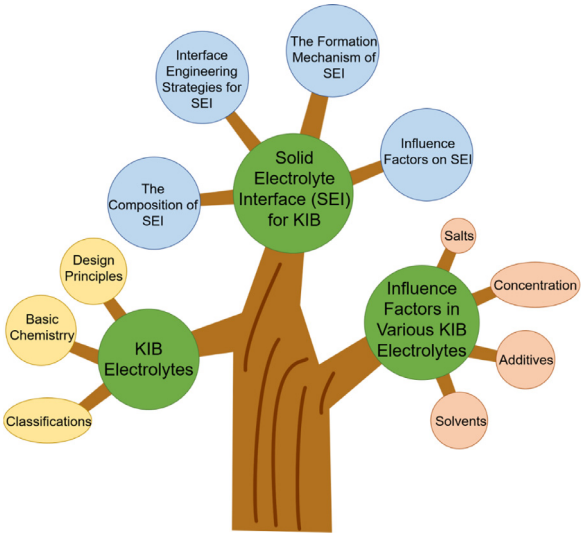

Figure 2. Schematic illustration of main components related to the KIB electrolytes and SEI.

Figure 3a. When discharging, K^+ is extracted from the negative electrode and inserted into the positive electrode through the electrolyte. Meanwhile, electrons pass from the negative electrode to the positive electrode through the external circuit. The charging process is just the opposite of discharging.

In fact, the reversible oxidation and reduction reactions of electrode materials are closely related to the electrolytes. Electrolyte is usually ion-conducting but electronically insulating, which consists of salts as carriers and solvents as transmission medium. Therefore, the electrolyte undertakes the task of transferring ions inside the battery to ensure the normal operation of battery. Both positive and negative electrodes react complicatedly with the electrolytes during the charge and discharge processes. Especially, as the voltage changes, the electrolyte will undergo an electrochemical decomposition reaction and the formation of a passivation layer on electrode surface during the first cycle. The composition and structure of the interfaces directly affect the electrochemical performance of battery.

Herein, Figure 3b demonstrates the formation mechanism of the passivation film from the energy level [32–34]. When the lowest unoccupied molecular orbital (LUMO) of the electrolyte is lower than the Fermi level of the negative electrode, electrons in the negative electrode will be transfered into the LUMO, leading the electrolyte to be reduced. By contrast, when the highest occupied molecular orbital (HOMO) is higher than the Fermi level of the positive electrode, electrons will be transfered into the positive electrode, causing the electrolyte to be oxidized. During the cycles of the battery, the potassium salt or solvent in electrolyte is reduced or oxidized, and the resulting material will deposit on the electrode surface to form a passivation film (SEI and cathode solid electrolyte interphase (CEI)). Similar to LIB and SIB, SEI layer of most the KIB anode materials forms spontaneously below 1.0 V in organic electrolytes [29,35,36].

2.2. Classifications of KIB Electrolytes

The KIB electrolytes can be divided into two main types: liquid electrolytes and solid electrolytes. Liquid electrolytes include organic system, aqueous system, and ionic liquid system, while solid electrolytes include inorganic solid system and polymer system.

Organic electrolytes are currently the most widely applied in KIB due to high ionic conductivity, good electrochemical stability, good compatibility with electrodes, and significant power density (**Figure 4a**). They are composed of K salts, organic solvents, and additives. Herein, the main advantages of organic electrolytes for KIB are summarized as follows. First, the relatively large dielectric constants of organic solvents are beneficial to the dissociation of K salts. Second, the low viscosity of organic solvents promotes rapid migration of K^+. Third, the chemistry and electrochemistry of organic electrolytes are relatively stable within a certain voltage range. Fourth, a stable passivation layer can be formed on electrode surface in organic electrolytes. However, organic electrolytes pose a major safety hazard owing to the flammability and volatilization of organic solvents. In addition, the reaction between highly active K metal and carbonate electrolyte results in poor CE. **[37]**

Aqueous electrolytes have also received extensive research in recent years owing to their high stability, high safety, low cost, and environmental friendliness (**Figure 4b**). They are usually made up of K salts, water solvent, and additives. First, aqueous batteries fundamentally avoid the safety problems caused by flammable organic electrolytes. Second, the cost of aqueous electrolytes is lower than other systems. Third, aqueous electrolytes own higher ionic conductivity than that of organic electrolytes. Fourth, water solvent is harmless and non-toxic to the environment. Nevertheless, the problem of aqueous KIB is the narrow voltage window, resulting in low energy density.

IL electrolytes in KIB have recently received continuous attention and are a promising type of electrolytes. They are comprised of organic anions and cations, coupled with K salt, demonstrating superior thermal and electrochemical stability, low volatility, and low flammability (**Figure 4c**). These features can enable KIB to achieve high energy density and improved safety. However, IL electrolytes have higher viscosity, lower ionic conductivity, and lower charge transfer numbers. It is precisely because of the increase in ion correlation that larger clusters are not conducive to transport, thus causing slow diffusion. **[38]** Increasing the operating temperature of battery can be expected to improve the diffusion coefficient. In addition, the high synthesis cost of IL electrolytes cannot be ignored.

Unlike organic electrolytes, solid electrolytes exhibit high safety, good mechanical properties, and excellent thermal stability (**Figure 4d**). Besides, solid electrolytes can support the battery to operate under extreme conditions (low and high temperature), while liquid electrolytes will deteriorate in the same condition. **[39]** In addition, solid electrolytes are expected to notably increase the energy density of batteries. However, several major challenges hinder the development of solid KIB. The solid electrolytes can effectively suppress dendrites formation due to its mechanical rigidity, but whether the influence of dendrites can be completely ignored is questionable. Besides, the stability of the interface between the electrode material and the solid electrolyte plays a critical role in the electrochemical performance of KIB. Thus, it is indispensable to develop effective strategies to alleviate the physical contact problem of solid electrolytes to improve ionic conductivity.

In general, in view of the characteristics of these four electrolytes, they can be used flexibly according to actual needs in the future to give full play to their greatest advantages.

2.3. Design Principles of KIB Electrolytes

According to advanced experience of LIB/SIB electrolytes, the main required characteristics of KIB electrolytes are proposed as follows:

(1) High Ionic Conductivity

The ionic conductivity of electrolyte depends on the lattice energy of the salt, viscosity and dielectric constant of solvent, and solvation effect (Figure 5a). The low lattice energy of salt means that the dissociation energy is low, which promotes the dissolution of K salt. Besides, the solubility of K salt in solvents is limited due to weak chemical bonds with the solvent molecules. Then, low viscosity and high dielectric constant of solvents facilitate ion diffusion [40]. Moreover, the solvation effect of K^+ in organic solvents affects ionic conductivity because the desolvation process determines the rate of ion migration and reaction. Lower desolvation energy leads to more convenient desolvation and higher ion diffusion rate. In addition, the solvation structure of K^+ and solvent molecules is also affected by the concentration of salts in electrolytes.

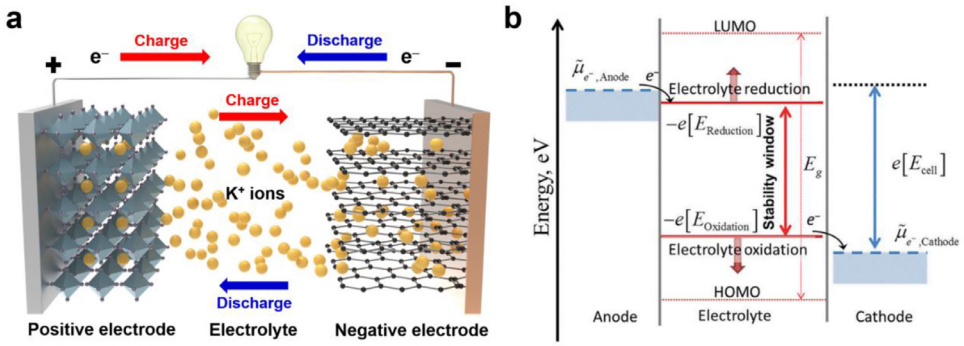

Figure 3. (a) Schematic configuration of KIB. (b) The energy state of the electrode and the electrolyte leads to the formation of a passivation film on the interface between the electrode and electrolyte. Reproduced with permission [32]. Copyright 2018, The Royal Society of Chemistry.

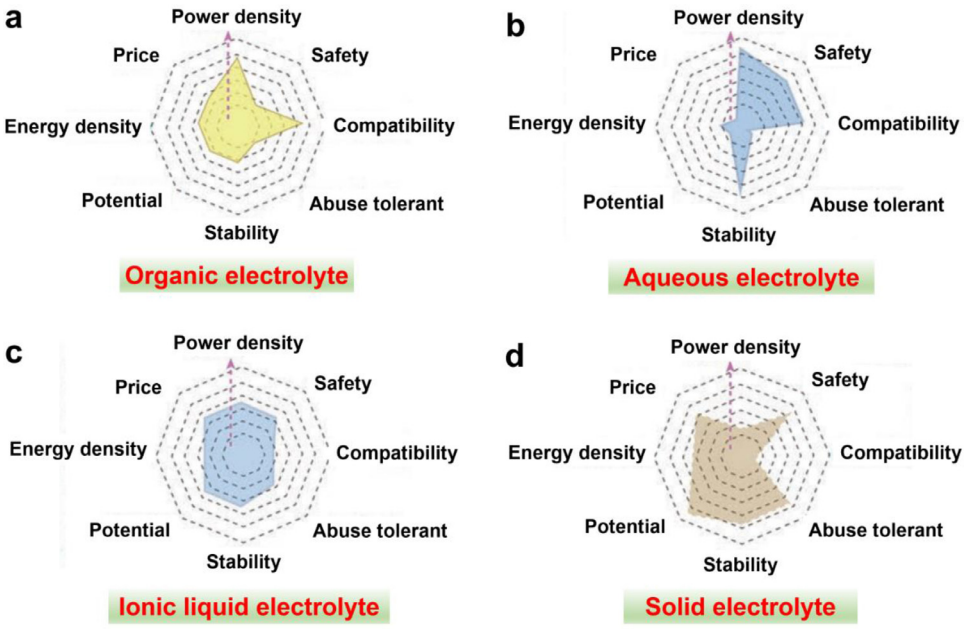

Figure 4. Main properties of four KIB electrolytes. Reproduced with permission [14]. Copyright 2019, Wiley-VCH.

The ionic conductivity of electrolyte exhibits a convex parabolic change as the concentration increases due to the number of free ions and electrostatic interference.

(2) Excellent Chemical and Electrochemical Stability

The chemically stable electrolytes should not react other components of battery, including current collector, separator, binder, and outer packaging materials, etc. (Figure 5b). However, certain electrolyte components (FSI^- and Ca^{2+}) are corrosive to the current collector or steel shell, which will cause the battery to fail [41,42]. On the other hand, wide electrochemical stability window (ESW) and stable electrode/electrolyte interface are required in electrochemical stable electrolytes, expecting to achieve high energy density and long cycle life of battery (Figure 5c). It is found that the composition and concentration affect the voltage window in organic electrolytes [43]. Also, the IL or solid electrolytes can significantly increase the width of ESW [44,45]. In addition, adjusting the electrolyte composition, concentration and additives can enhance the electrochemical stability of passivation layer.

(3) Good Interface Contact

The interface problem between solid-liquid and solid-solid contact mainly involves the resistance, growth of dendrites and compatibility between electrolyte and electrode. Good wettability is beneficial to the total contact between liquid electrolyte and electrode material, reducing the charge transfer resistance **(Figure 5d)**. The disadvantage of solid electrolytes is poor contact with isolated particles of active material, resulting in higher resistance. However, liquid electrolytes are subject to safety issues caused by K dendrites, while solid electrolytes with the excellent mechanical strength can effectively inhibit the K dendrites growth and improve battery safety. **[45]** Typically, a passivation layer formed on electrode surface improves the interface compatibility in liquid electrolytes, but it will reduce the initial CE (ICE) of battery. In addition, artificial interface engineering can improve this compatibility problem in solid electrolytes.

(4) Wide Range of Applicable Temperature

The electrolyte is the most flammable component in battery, which greatly affects the battery safety. The high thermal stability of electrolytes means that they will not freeze or decompose even in a low temperature and high temperature environment **(Figure 5e)**. Thus, thermodynamically stable K salts, non-flammable solvents, and flame-retardant additives are required for safe electrolytes. Fortunately, the decomposition temperature of some K salts is usually higher than those of Na/Li salts **(Table 1)**. Moreover, it is well known that non-flammability and safety are the advantages of aqueous and solid electrolytes. In addition, IL electrolytes show high thermal stability due to its low flammability. In addition, it is feasible to add flame-retardant solvents to conventional electrolytes to obtain higher safety **[46]**.

(5) Environmentally Benign and Low Cost

A good electrolyte should possess the characteristics of environmental friendliness and low cost, which are conducive to its practical application **(Figure 5f)**. The environmental damage and high cost should be avoided. In addition to high energy density and long lifespan KIBs, organic electrolytes and IL electrolytes should also be improved by decreasing cost. Especially, aqueous electrolytes and solid electrolytes are likely to become the development trend of next-generation electrolytes due to their green methods and low-cost advantages.

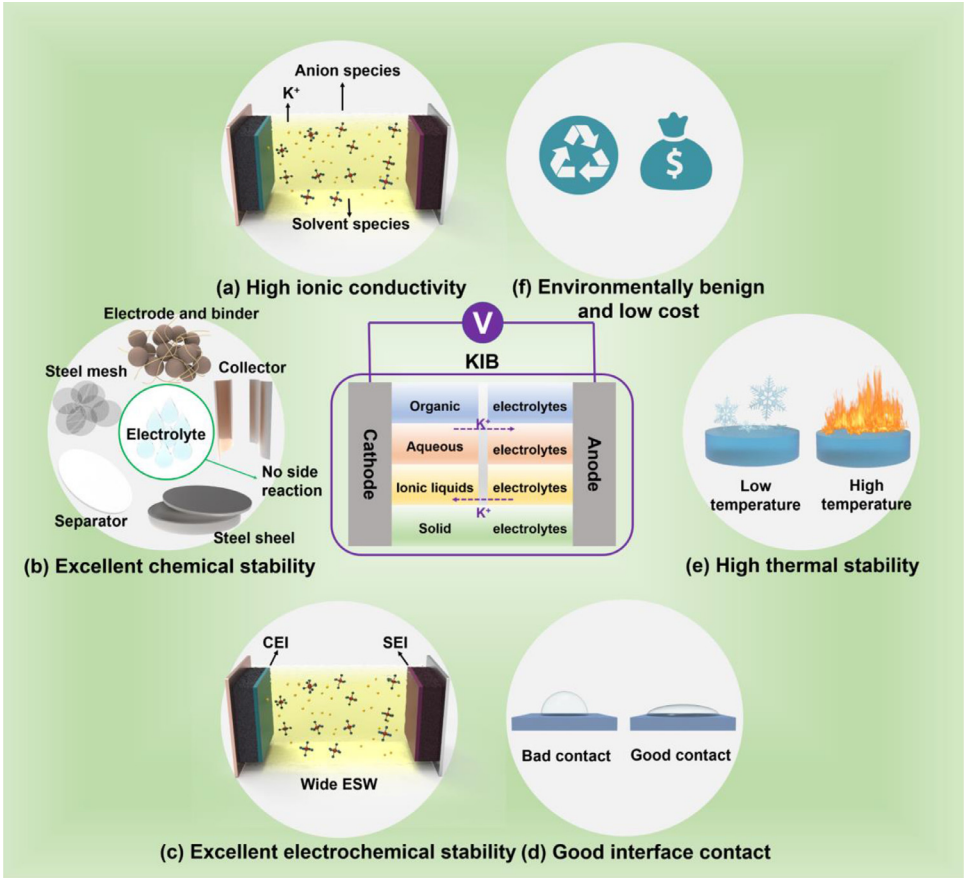

Figure 5. The main properties of high performance KIB electrolytes, involving (a) high ion conductivity, (b) excellent chemical stability, (c) excellent electrochemical stability, (d) good interface contact, (e) wide range of applicable temperature (good thermal stability and low freezing point), and (f) environmentally friendly and low cost.

Table 1
Physical and chemical properties of the reported K salts for KIB electrolytes.

K Salts	Chemical structures	Molar mass (g mol^{-1})	Decomposition temperature (Tm) [°C] (Na and Li salts)	Conductivity (σ)a) [mS cm^{-1}] (Na and Li salts)	Solubility	Cost	Toxicity	Ref.
KPF_6	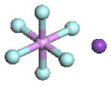	184.06	575 (300, 200)	5.75 (7.98, 5.8)	0.9 mol kg^{-1} in PC; 1.8 mol kg^{-1} in DME	Low cost	Low toxicity	[40]
KBF_4	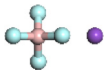	125.90	530 (384, 293)	0.2(/, 3.4)	Hardly dissolved in PC	Highly cost	Highly toxic	[40]
$KClO_4$	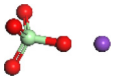	138.55	610 (468, 236)	1.1(6.4, 5.6)	Hardly dissolved in PC	Low cost	Highly toxic	[40]
KFSI	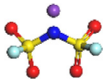	219.23	102 (118, 130)	7.2(/)	10 mol kg^{-1} in PC; 7.5 mol kg^{-1}in DME; 12 mol kg^{-1} in GBL	Highly cost	Nontoxic	[40]
KTFSI		319.24	198-203 (257, 234)	6.1(6.2, 5.1)	6 mol kg^{-1} in DME	Highly cost	Nontoxic	[40]
KCF_3SO_3	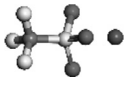	188.17	238.5 (248, >300)	(/, 1.7)	22 mol L^{-1} in water	Highly cost	Nontoxic	[98]

3. Influence Factors in Various KIB Electrolytes

3.1. Organic Liquid Electrolytes for KIB

The performance of organic electrolytes is deeply affected by three major components (K salts, solvents, and additives) and concentrations. Therefore, their effects on battery performance will be discussed from four aspects in the following sections.

3.1.1. The Effect of K Salts

K salt is one of the three major components of KIB electrolytes, which is closely related to the electrochemical properties of electrolytes. The

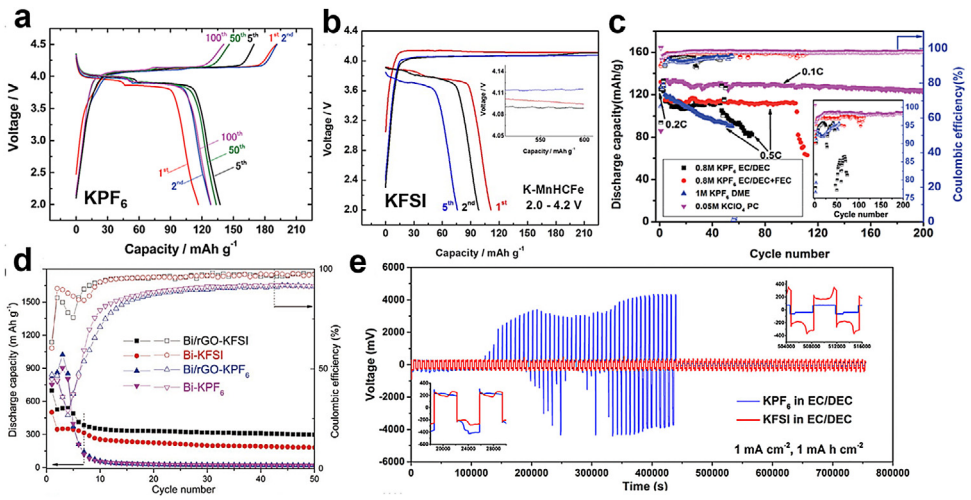

Figure 6. Effect of K salts in electrolytes. Charge/discharge curves of K-MnHCFe in (a) KPF_6-based (2.0-4.5 V) and (b) KFSI-based (2.0-4.2 V) electrolytes. Reproduced with permission [47]. Copyright 2017, The Royal Society of Chemistry. (c) Cycling performance of KFeHCF in the KPF_6 and $KClO_4$-based electrolytes. Reproduced with permission [48]. Copyright 2017, The Royal Society of Chemistry. (d) Cycling performance of Bi-based electrodes in KPF_6 and KFSI-based electrolytes. Reproduced with permission [49]. Copyright 2018, Wiley-VCH. (e) Voltage profiles of K-K symmetric cells in KPF_6 and KFSI-based electrolytes. Reproduced with permission [52]. Copyright 2018, Elsevier Ltd.

following points need to be paid attention to when choosing the suitable K salt. First, high solubility in solvents increases the concentration of K^+ in the electrolyte. Second, good electrochemical stability of K salt determines ESW. Third, good chemical stability of K salt reduces the occurrence of its side reactions. Fourth, excellent thermal stability of K salt will improve the safety of the battery. Fifth, low-cost and non-toxic K salts are conducive to industrialization. Unfortunately, the types of K salts that have been reported so far are rare. The main K salts in KIB electrolytes include KPF_6, $KN(SO_2F)_2$ (KFSI), $KN(CF_3SO_2)_2$ (KTFSI), KBF_4, $KClO_4$, and KCF_3SO_3. In **Table 1**, some physicochemical properties of the most used K salts for KIB electrolytes are summarized.

Owing to no corrosion on the Al current collector, high ionic conductivity, good compatibility, and low cost, KPF_6 has been widely used in performance testing of cathodes and anodes of KIB. However, KPF_6 is extremely sensitive to water and oxygen, and it is prone to hydrolysis reaction to produce HF, PF_5, and POF_3 in contact with water. Other common K salts are KFSI and KTFSI, which display higher conductivity in PC-based electrolytes. **[40]** Nevertheless, the issue of FSI^- and $TFSI^-$ lies in the corrosion of the Al collector at high voltage. Besides, the strong interaction between K^+ and BF_4^- makes KBF_4-based electrolyte poorly conductive. $KClO_4$ is rarely used because of its strong oxidation. The problem of KCF_3SO_3-based electrolyte is also poor conductivity.

K^+ makes K salts show some different properties from Li and Na salts. For instance, the melting points of KPF_6, KBF_4, and $KClO_4$ are higher than those of Na and Li salts, manifesting higher thermal stability and better safety of these K salts. The ionic conductivity of these K salts is lower than that of the corresponding Na and Li salts, which is ascribed to large size and low Lewis acidity of K^+.

Komaba *et al.* compared KFSI, KTFSI, KPF_6, KBF_4, and $KClO_4$ in PC and measured their ionic conductivity. **[40]** Whether in EC/DEC system or PC system, the solubility of KBF_4 and $KClO_4$ salts is relatively small, while the solutions of KFSI, KTFSI, and KPF_6 show their high solubility. The ionic conductivity of KFSI, KTFSI, and KPF_6 solutions is much higher than that of KBF_4 and $KClO_4$. Moreover, KFSI was found highly soluble in various solvents (10 mol kg^{-1} in PC, 7.5 mol kg^{-1} in dimethoxyethane (DME), 12 mol kg^{-1} in γ-butyrolactone (GBL)). The KFSI-DME system showed the highest ionic conductivity, which can be attributed to the low Lewis basicity of FSI^-, resulting in a weak interaction between anions and cations. In addition, the 7 mol kg^{-1} KFSI-DME solution exhibits lower viscosity than other high-concentration electrolytes (10 mol kg^{-1} KFSI-PC and 12 mol kg^{-1} KFSI-GBL).

Recently, researches on the effects of different K salts on electrode performance have shown an increasing trend. Each K salt has different effects on the K storage of electrode materials due to its own characteristics. KPF_6 is confirmed to be more suitable in the high-voltage cathodes than KFSI. It is found that $K_{1.75}Mn[Fe(CN)_6]_{0.93}$•$0.16H_2O$ (K-MnHCFe) presents high platforms (4.08, 4.11, 3.97, and 3.89 V) and a high capacity (137 mA h g^{-1}) in KPF_6-based electrolyte **(Figure 6a)**. In contrast, K-MnHCFe in KFSI-based electrolyte exhibits large voltage polarization, severe overcharging, and a rapid capacity decay **(Figure 6b). [47]** This phenomenon can be attributed to the corrosion of Al foil by FSI^- at high potential. Besides, $KClO_4$ may effectively suppress the side reactions between the electrolyte and K metal. Compared with KPF_6-based electrolytes, the cell in $KClO_4$-based electrolytes exhibits higher CE (~98.5%) and long-term stability (a capacity retention of 92.8% after 200 cycles at 0.1C) **(Figure 6c). [48]** The excellent cycling performance can be related to the strong oxidation of $KClO_4$, which can react with K to form a robust SEI, avoiding the occurrence of side reactions.

KFSI can promote the formation of stable SEI. It is found that Bi/reduced graphene oxide (Bi/rGO) electrode exhibits higher capacity, higher CE, and more stable cycling ability in KFSI-based electrolyte than those in KPF_6-based electrolyte **(Figure 6d). [49]** The advantages of the KFSI-based electrolyte are demonstrated in other alloyed materials (Sn, Sb, GeP_5, Sn_4P_3, and red P (RP)), **[**[49,50,52,53]**]** transition-metal dichalcogenide (MoS_2, $NiCo_{2.5}S_4$, and $MoSe_2$), **[**[54–56]**]** nitrogen-doped graphite foams (NGFs) and K metal. **[53,57]** The improved cycling life is related to the FSI^-, which plays a role in preventing the electrolyte decomposition, modifying the interface, and forming stable SEI. On the other hand, KFSI can efficiently inhibit the growth of K dendrites and suppress the occurrence of some side reactions. For instance, the battery in KFSI-based electrolyte can maintain stable operation for a long time, while a short circuit occurs shortly after running in the battery of KPF_6-based electrolyte **(Figure 6e). [52]** The short circuit phenomenon is probably due to the growth of K dendrites and the continuous generation of SEI. Moreover, it is also confirmed that the stronger solvation occurs in KFSI-based electrolyte. Guo *et al.* investigated the interaction between salts and solvents, finding that the peaks proportion and strengths of the K^+ solvated molecules in KFSI-based electrolyte were much higher than those in KPF_6-based electrolyte. **[53]** Therefore, the free solvent molecules in the electrolyte will be greatly reduced, which is helpful to avoid the occurrence of side reactions.

In addition to single-salt electrolytes mentioned above, a type of binary-salts electrolyte also be developed recently. Komaba *et al.* developed a KPF_6-KFSI-based electrolyte for long-term stability, high-voltage KIB. **[58]** They found that KPF_6-KFSI-based electrolyte shows higher ionic conductivity than KPF_6-based electrolyte. This electrolyte with a KPF_6-KFSI molar ratio more than 3 has strong oxidation stability, which solves the corrosion issue of the Al current collector by KFSI. An ICE of 72.5%, a high capacity of 105 mA h g^{-1} and a high capacity retention of 75% after 500 cycles are delivered in $0.75KPF_6$-0.25KFSI-based electrolyte. Such excellent cycling performance in the full KIB can be at-

tributed to the decomposition products of FSI^- which stabilizes the SEI on the graphite electrode.

3.1.2. The Effect of Solvents

Solvent is one of three major components of electrolyte, which affects the properties of electrolytes. The ideal electrolyte solvent should have the following characteristics. First, solvents with high dielectric constants can dissolve enough K salts. Second, low viscosity of solvents is good for K^+ transport. Third, solvents with high boiling point (Tb) and low melting point (Tm) enable electrolyte have a wide operating temperature window. Fourth, high flash point (Tf) of solvents ensures the safety of battery. Fifth, the solvents with wide ESW and stability can enable the positive and negative materials perform their extreme functions. Finally, environmentally-friendly and low-cost are required for solvents. The most important properties of organic solvents are listed in **Table 2**. It is found that the organic solvent family studied in KIB is basically the same with that used in LIB and SIB, including esters and ethers.

Ester solvents are the main solvents in KIB due to its higher electrochemical stability and ability to dissolve K salts. The commonly used are the cyclic EC, PC, GBL, and fluoroethylene carbonate (FEC), and the linear DEC, ethyl methyl carbonate (EMC), dimethyl carbonate (DMC), triethyl phosphate (TEP), dimethyl methyl phosphonate (DMMP), and trimethyl phosphate (TMP), etc. Besides, ether solvents exhibit low dielectric constant and low viscosity, while their active properties and poor oxidation resistance limit their applications. The common ether solvents include cyclic 1,3-dioxacyclopentane (DOL), the linear DME, triethylene glycol dimethyl ether (TEGDME), and diethylene glycol dimethyl ether (DEGDME). Most K^+ electrolyte formulations refer to dissolving a K salt in a mixture of one, two or more solvents.

The interaction of K^+ with organic solvents has been theoretically studied and compared with Li^+, Na^+, and Mg^{2+}. **[18]** Among the four ion species, K^+ exhibits the lowest ion-solvent interaction energy, which is related to high-rate capability of KIB. In this regard, the small activation energy for desolvation leads to low interface reaction resistance, and the small solvation ion radius causes the high ion conductivity of the K^+. Nevertheless, the weak ion-solvent interaction leads to the low solubility of K salt. In addition, the analysis on the interaction energy between solvents and ions shows that the polarization and electrostatic interactions in the K complex are the smallest, which explains that the K^+ radius is the largest and the Lewis acidity is the lowest among them. Furthermore, it is found that TMP, dimethyl formamide (DMF), N-methyl oxazolidinone (NMO), dimethyl imidazolidinone (DMI), and N-methyl pyrrolidinone (NMP) have strong interactions with K^+. These solvents are expected to dissolve more K salts, which are promising in the choice of solvents in the future of KIB.

The effect of organic solvents on electrode material has been evaluated in recent years. It is found that EC/PC-based electrolytes are more suitable for both high voltage and low voltage. Komaba *et al.* reported the high-voltage behavior (2.0-5.0 V) of $KVPO_4F$ and $KVOPO_4$ in EC/DEC and EC/PC-based electrolytes. **[59]** A discharge capacity of ~80 mA h g^{-1} and the discharge voltage of 4.13 V for $KVPO_4F$ were achieved in EC/PC-based electrolytes. Besides, the irreversible capacity of $KVPO_4F$ at the initial cycle in EC/PC-based electrolytes is less than that in EC/DEC-based electrolytes (**Figure 7a and b**). The reason is that the irreversible anodic current of EC/PC-based battery in the high-potential range is much smaller than that of EC/DEC-based battery. Thus, the side reactions of cathodes at high voltage can be efficiently suppressed in EC/PC-based electrolytes. The same phenomenon occurs in graphite anode. Xu *et al.* analyzed the effect of different solvents (EC/PC, EC/DEC, and EC/DMC) on the K storage performance of graphite. **[60]** The EC/PC system exhibits high ICE and stable cycling ability (**Figure 7c**). The decomposition of DEC and DMC at low potential may cause great amount irreversible capacity. Especially, the rapid capacity decay of EC/DMC system is probably due to the continuous decomposition of DMC and the formation of unstable SEI. **[61,62]**

TEP solvent can protect the layered structure of the electrode. **[63]** The $K_{0.5}MnO_2$ cathode pre-cycled in TEP-based electrolyte is highly efficient, while the fast capacity decay is exhibited when used in EC/DEC-based electrolyte (**Figure 7d**). It is claimed that passivation layer is not a decisive factor leading to different K storage performance of $K_{0.5}MnO_2$ cathode in EC/DEC and TEP-based electrolytes. They found that EC molecules are embedded in the layers due to the relatively weak interaction with K^+ when $K_{0.5}MnO_2$ cathode is deeply charged. The co-intercalation will destroy the layered structure, which leads to capacity decay. However, TEP can avoid molecular embedding with the relatively large the Sterimol parameters ($D_{K\text{-}M}$) values (4.53 Å), thus protecting the layered structure, enabling the battery to cycle stably at high voltage (4.2 V). Besides, TEP-based electrolyte demonstrated the highest ICE (88.45%) and the smallest overpotential (0.4 V) among the three phosphate electrolytes (**Figure 7e**). **[46]** This can be ascribed to the high ionic conductivity and low viscosity of TEP-based electrolyte, because K^+ has a weak solvation effect in TEP solution. In addition, the flame-retardant properties of TEP could address the battery safety problem.

FEC enables $KVPO_4F$ cathode with reversible cycling performance at high voltage of 4.9-5.0 V. **[64]** Nikitina *et al.* compared the electrochemical behaviors of $KVPO_4F$ cathode in tetramethylene sulfone (SL), adiponitrile (ADN), and FEC-based electrolytes. It is found that FEC-based electrolyte is more attractive for high voltage with lower charge transfer resistance than SL and ADN-based electrolytes, which is ascribed to the easiness formation of stabilizing surface protective films in FEC-based system. Moreover, the capacity of $KVPO_4F$ is highly reversible at 4.9 V and slightly decayed at 5.0 V in FEC-based system (**Figure 7f**).

Ether solvents have greater solubility for K salts, which are different from ester solvents. Recently, ether electrolytes exhibit significant superiority when used in anode materials (graphite, alloyed materials, organic materials, and K metal, etc.). Obviously, the K storage mechanism of graphite anode in ether-based electrolytes varies from that in carbonate-based electrolytes. For instance, the electrochemical performances of graphite anode in DME and EC/DMC-based electrolytes are comparatively investigated. **[65]** The capacities of 82 mA h g^{-1} in DME-based electrolytes and 8 mA h g^{-1} in EC/DMC-based electrolytes at 10 C are formed in a sharp contrast, which may be ascribed to the low interaction force caused by a charge shielding effect in DME-based electrolytes (**Figure 8a**). Moreover, it should be noted that the K^+ intercalates into graphite in EC/DMC-based electrolyte, while the K^+-ether co-intercalation in DME-based electrolyte. The co-intercalation behavior avoids the slow desolvation process, which enables the fast kinetics of graphite.

DME could effectively protect organic electrode materials. The cycling stability of anthraquinone-1,5-disulfonic acid sodium salt (AQDS) cathode in EC/DEC and DME-based electrolytes was compared. **[66]** Improved cycling stability is demonstrated in DME-based electrolyte, which is ascribed to the robust SEI layer with fast reaction kinetics (**Figure 8b**). Meanwhile, the excellent electrochemical performance of dipotassium terephthalate (K_2TP) anode also benefits from DME solvent. **[67]** A high CE (90%) and much less polarization of poly (anthraquinonyl sulfide) (PAQS) cathode are achieved in DOL/DME-based electrolyte. **[68]**

DME is more compatible with alloy anodes (Sn, Bi, and SnSb) than ester solvents. When micrometer-sized Bi is used as an anode for KIB, the capacity retention of 94.4% in DME-based electrolyte can be achieved, which is superior to that in PC-based electrolyte (**Figure 8c**). **[69]** It is concluded that compatible electrolytes can stabilize the powdered fresh interface caused during the charging/discharging process. In incompatible electrolytes, SEI does not prevent the decomposition of electrolyte. In addition, a remarkable ICE (90.1%) of the 3D SnSb electrode is obtained in DME-based electrolyte. **[70]**

It is found that DME-based electrolyte can effectively passivate the K metal surface, forming stable and uniform SEI. **[43]** A highly reversible and long-term stable K plating-stripping is obtained only in KFSI-DME

Table 2
Physical and chemical properties of the reported organic solvents for KIB electrolytes [14,25]

Solvent	Chemical structure [cP]	Melting point (Tm) [°C]	Boiling point (Tb) [°C]	Flash point (Tf) [°C]	Viscosity (η) at 25°C	Dielectric constant (ε) at 25°C
EC	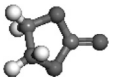	36.4	248	160	2.1	89.78
PC	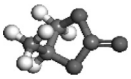	-48.8	242	132	2.53	64.92
DMC	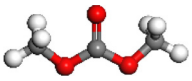	4.6	91	18	0.59 (20°C)	3.1
EMC	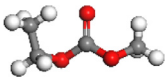	-53	110	/	0.65	2.96
DEC	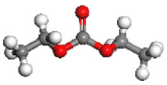	-74.3	126	31	0.75	2.8
FEC	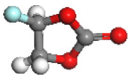	18	249	120	2.35	/
TEP	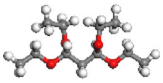	-56.4	215	117	1.6	/
TMP	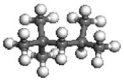	-46	197	148	1.3	/
DMMP	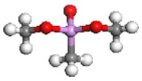	-50	181	104	1.75	/
GBL		-43.53	204	98.3	1.7	39 (20°C)
ADN	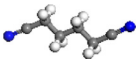	1	295	/	6.1	30
VC	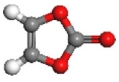	22	162	73	2.23	/
DME	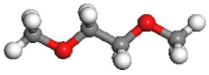	-58	84	0	0.46	7.2
DEGDME	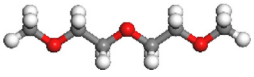	-64	162	57	1.06	7.18
TEGDME	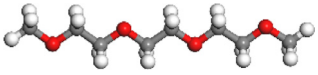	-46	216	111	3.39	7.53
DOL	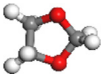	-95	75.6	1	0.6 (20°C)	/

electrolyte, while fast capacity decay and low CE are demonstrated in KPF_6-DME, KTFSI-DME, and KPF_6-EC/DEC electrolytes, respectively (**Figure 8d**).

In addition to the application of DME-based electrolytes in anode electrodes, the application of cathode electrodes is also involved. [71] A higher capacity and better cycling ability of TiS_2 cathode are presented in DME-based electrolyte. Besides, the galvanostatic intermittent titration technique (GITT) demonstrated that the same K storage mechanism of TiS_2 in both EC/DMC and DME-based electrolytes. However, high K^+ diffusion coefficient and better kinetics in charge transfer are provided by DME-based electrolyte (**Figure 8e**).

As other ether solvents, DEGDME has received more attention in recent years. DEGDME-based electrolyte is found to be more stable than EC/DEC. [72] More by-products were found in EC/DEC system, which may be caused by electrolyte decomposition. The decomposition products of DEC may be K ethyl and carbonates. However, no obvious changes occurred in DEGDME-based system, indicating that the DEGDME is relatively stable. The fast capacity decay of graphite anode

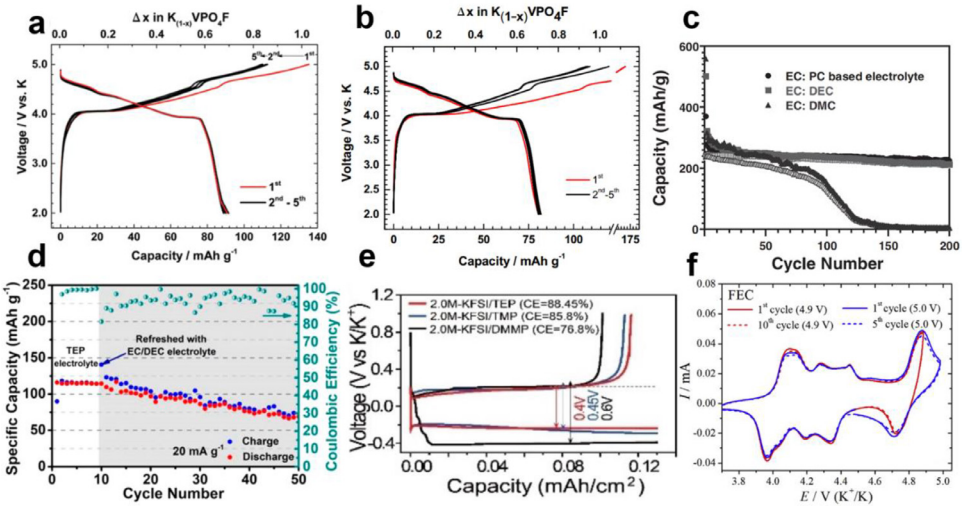

Figure 7. Effect of esters in electrolytes. Charge/discharge curves of $KVPO_4F$ (2.0-5.0 V) in (a) EC/PC and (b) EC/DEC-based electrolytes. Reproduced with permission [59]. Copyright 2017, The Royal Society of Chemistry. (c) Cycling performance of graphite anodes in EC/PC, EC/DEC, and EC/DMC-based electrolytes, respectively. Reproduced with permission [60]. Copyright 2016, Wiley-VCH. (d) Cycling performance of $K_{0.5}MnO_2$ cathode cycled in TEP-based electrolyte initially, then in EC/DEC-based electrolyte. Reproduced with permission [63]. Copyright 2020, American Chemical Society. (e) Initial K plating and stripping behavior of K/Cu half cells in TEP, TMP, and DMMP-based electrolytes, respectively. Reproduced with permission [46]. Copyright 2020, Wiley-VCH. (f) Cyclic voltammogram (CV) curves of $KVPO_4F$ cathode in SL, ADN, and FEC-based electrolytes, respectively. Reproduced with permission [64]. Copyright 2017, Elsevier Ltd.

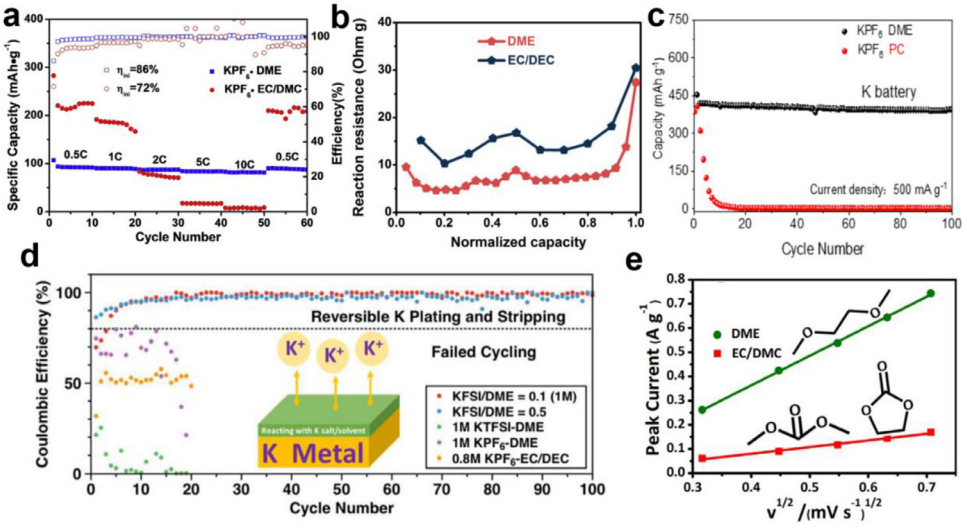

Figure 8. Effect of ethers in electrolytes. (a) Rate ability of graphite anode in DME and EC/DMC-based electrolytes. Reproduced with permission [65]. Copyright 2019, Elsevier Ltd. (b) Reaction resistance of K^+ in EC/DEC and DME-based electrolytes during cycles. Reproduced with permission [66]. Copyright 2018, Wiley-VCH. (c) Cycling performance of Bi anode in PC and DME-based electrolytes. Reproduced with permission [69]. Copyright 2020, American Chemical Society. (d) Comparison of galvanostatic K plating-stripping in various electrolytes. Reproduced with permission [43]. Copyright 2017, American Chemical Society. (e) Peak current versus square root of scan rates of TiS_2 cathode CV in DME and EC/DMC-based electrolytes. Reproduced with permission [71]. Copyright 2018, American Chemical Society.

in EC/DEC electrolyte is ascribed to the continuously thickening SEI due to the decomposition of electrolyte. Furthermore, the K^+-solvent co-intercalation mechanism of graphite anode in KCF_3SO_3-DEGDME electrolyte is revealed by the experimental results and first-principles calculations. **[73]** A sluggish desolvation process is avoided during the $[K\text{-DEGDME}]^+$ complex intercalation, which is a cause of the fast kinetics.

3.1.3. The Effect of Additives

Additives refer to adding a small amount of other components to the original electrolyte system to change the target characteristics of the electrolyte. The typical role of additives in LIB and SIB has already been confirmed to modify SEI, increase surface wettability, improve flame retardancy, reduce viscosity, improve solvent solubility, and prevent overcharging. [74–79] Thus, the development of electrolyte additives is also an important hotspot in research of KIB. Currently, KIB electrolyte system has its own shortcomings, such as low CE, poor cycle life, poor high voltage resistance, temperature limitations, and safety issues. In this regard, the application of electrolyte additives is the simplest and most effective way to solve these problems and improve the performance of KIB. Meanwhile, the ideal KIB additives should reduce irreversible capacity, increase cycle life, inhibit the dissolution of cathode materials, reduce gas generation, prevent overcharge, and improve the thermal stability of K salts and organic solvents.

Up to now, the research on KIB electrolyte additives is rare. However, there have been some studies on the influence of additives on KIB in recent years. FEC has been confirmed to play different roles in different battery systems. FEC can effectively improve the CE of cathode materials. **[37,47]** By adding different concentrations of FEC additive (2 and 5%), the CE and cycle life of $K_{1.69}Fe[Fe(CN)_6]_{0.90}\cdot 0.4H_2O$ (KFeHCF-S) are significantly improved **(Figure 9a)**. Similar reports prove that 2 vol% FEC additive can improve the ICE of K-MnHCFe (from 61% to 90%), but it will play a negative role in cycling stability **(Figure 9b and c)**. This phenomenon is because FEC does not completely suppress the occurrence of side reactions.

Nevertheless, FEC also could exacerbate the occurrence of side reactions. It is found that the cycle performance and rate capability of GeP_5 anode become worse using KPF_6 and KFSI-based electrolytes with FEC. **[50]** The reason is that the solvation energy of electrolytes is greatly improved (from 0.305 eV to 1.281 eV) due to the presence of FEC. The larger solvation energy indicates that the interaction force between the solvent and K^+ is greater, making the diffusion of K^+ and desolvation more difficult **(Figure 9d)**. Similar electrochemical behavior also exists in Sn_4P_3 anode. **[52]** The color change of the separator in electrolytes

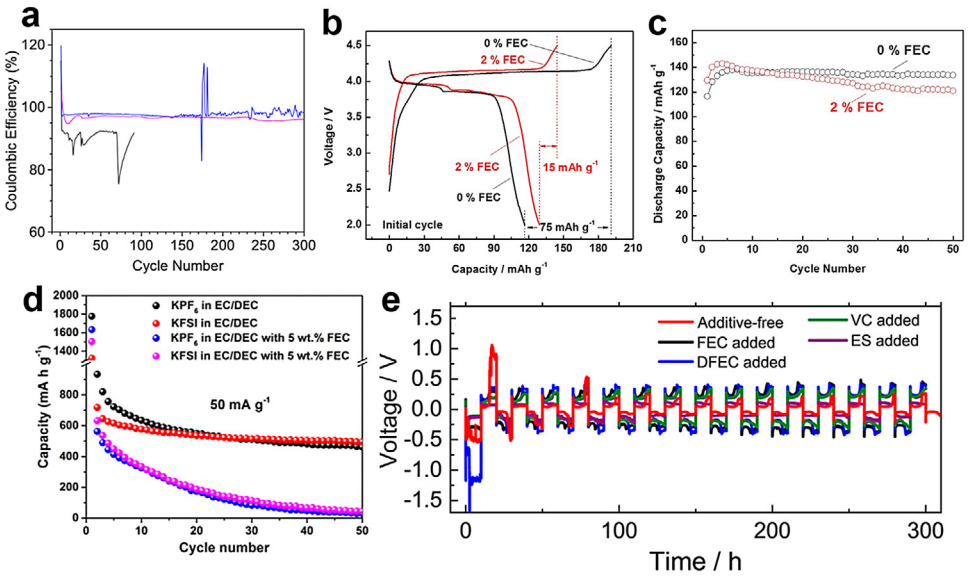

Figure 9. Effect of additives in electrolytes. (a) CE of KFeHCF-S cathode with no FEC (black), 2% (blue) and 5% (purple) FEC. Reproduced with permission [37]. Copyright 2017, American Chemical Society. (b) Initial charge-discharge curves and (c) cycling performance of K-MnHCFe cathode with 0% and 2% FEC. Reproduced with permission [47]. Copyright 2017, The Royal Society of Chemistry. (d) Cycling performances of GeP_5 anode with various electrolytes. Reproduced with permission [50]. Copyright 2018, Elsevier Ltd. (e) Cycling performances of symmetric K cells with or without FEC, DFEC, VC, or ES (1 vol%). Reproduced with permission [80]. Copyright 2019, American Chemical Society.

with FEC is more obvious than in electrolytes without FEC, indicating that more serious side reaction has occurred in electrolytes with FEC. **[55]**

Additionally, the presence of additives (FEC, difluoroethylene carbonate (DFEC), vinylene carbonate (VC), and ethylene sulfite (ES)) did not play a positive role in the plating/stripping of K metal. **[80]** Komaba *et al.* studies the effect of different additives on electrolytes. It is found that FEC, DFEC, and VC increased the polarization of the battery, while the presence of ES did not change the electrolyte obviously (**Figure 9e**).

In addition to the conventional additives mentioned above, some new additives for KIB have also been developed recently. Matsumoto *et al.* developed potassium difluorophosphate (KDFP) electrolyte additive to promote the generation of robust SEI on graphite, significantly improving the cycle life and CE of the battery. **[81]** A capacity retention (76.8%) over 400 cycles and the average CE (99.9%) of graphite are obtained in electrolyte with KDFP (0.2 wt%). It is the presence of KDFP that make SEI rich in KF and PO_x, thus the SEI and K overpotential are improved. Besides, Ming *et al.* introduced ethylene sulfate (DTD) additive for safe KIB electrolyte. **[82]** They found that DTD has a tremendous effect on the K storage performance of graphite, because it changed the solvation structure of K^+, which determines the interface behavior of K^+-solvent. It is particularly noteworthy that DTD can replace a part of TMP solvent and jointly build the first solvated shell of K^+.

3.1.4. The Effect of Concentration

The development of high-concentration electrolyte has become an efficient strategy to promote the electrochemical performance of batteries [83–86]. Thus, the application of high-concentration electrolytes in KIB is widespread, and their advantages are summarized as follows.

(1) Withstanding high voltage. The redox stability of high concentration electrolytes was analyzed by the linear sweep voltammetry (LSV). The position of the sudden increase of current curve is about 3.5 V in diluted electrolyte, but this potential will be delayed to 5.0 V in concentrated electrolyte (**Figure 10a**). **[43]** This means that diluted electrolyte is more likely to decompose than concentrated electrolyte. FSI^- mostly exists in the form of free anions in diluted electrolyte, while behaves more like solid state in concentrated electrolyte. Besides, the peak of DME solvent molecule gradually weakens as the concentration increases, while the solvation peak gradually increases. Meanwhile, the HOMO is reduced because the DME donates oxygen lone pair electrons to K^+, which effectively inhibits the oxidative decomposition of electrolyte. In addition, a high-energy-density (207 Wh kg^{-1}) graphite dual ion battery based on a high concentration electrolyte was presented. The high operating voltage of about 4.7 V in this battery system is unbearable for conventional traditional electrolytes. **[87]** Recently, the dual interface layer of the tough SEI film derived from the high concentration electrolyte and the inactive K-lean spinel interlayer enable $K_{0.67}MnO_2$ to achieve stable electrochemical performance in KIB. **[88]**

(2) Enhancing safety. The safety of the battery is an indispensable premise. It is particularly important to develop high safe electrolytes for KIB owing to highly active K metal. Generally, the traditional organic electrolyte is volatile and flammable, which makes the battery face the risk of ignition or even explosion. Adding flame retardants (TMP, TEP, and DMMP) to electrolyte is an effective way to improve battery safety in LIB and SIB. In view of this, Guo *et al.* reported a high concentration electrolyte using a flame retardant as a single solvent (2 M KFSI-TEP), which simultaneously improved the performance and safety of KIB. **[46]** Moreover, it can be found in the flame test that the electrolyte is easily ignited in 1.15 mol kg^{-1} KFSI-based electrolytes, but cannot be ignited in 6.91 mol kg^{-1} KFSI-based electrolytes (**Figure 10b**). **[**[89]**]**

(3) Alleviating the side reactions. The electrochemical performance of battery is affected by many side reactions (such as the corrosion of Al, the shuttle of polysulfide and so on). However, a greatly reduced number of free solvent molecules in high concentration electrolytes, which can effectively suppress side reactions. **[40]** It is found that the Al foil has been severely corroded in 2 mol kg^{-1}-based electrolyte, while the surface of the Al foil does not change obviously in 7 mol kg^{-1}-based electrolyte (**Figure 10c**). This phenomenon may be related to the low dielectric constant of DME solvent, which plays a decisive role in suppressing side reactions. In addition, high concentration electrolyte can efficiently suppress the dissolution and shuttle of polysulfide. The K-S battery is prone to overcharge in low concentration electrolytes, but this problem is effectively suppressed by increasing the electrolyte concentrations. **[**[90]**]** The highly reversible reaction of sulfur with a high concentration of 5 M electrolyte is achieved, which is ascribed to the effective suppression of polysulfide shuttle behavior (**Figure 10d**).

(4) Promoting uniform and stable SEI. **[**[91],[92]**]** It is found that most of SEI components formed in 3 M KFSI-based electrolyte are inorganic, while the SEI layers in 0.8 M KPF_6-based electrolyte are consisted of organic and inorganic components. Besides, the SEI maintains well after 2000 cycles in 3 M KFSI-based electrolyte, indicating its uniform and stability. The special interface and SEI formed in high concentration electrolytes enable the electrode materials exhibit excellent electrochemical performances in term of cycling stability and rate capability (**Figure 10e and f**).

In brief, the choice of salts, solvents, additives, and concentration was found to play a critical role in electrochemical performance of KIB.

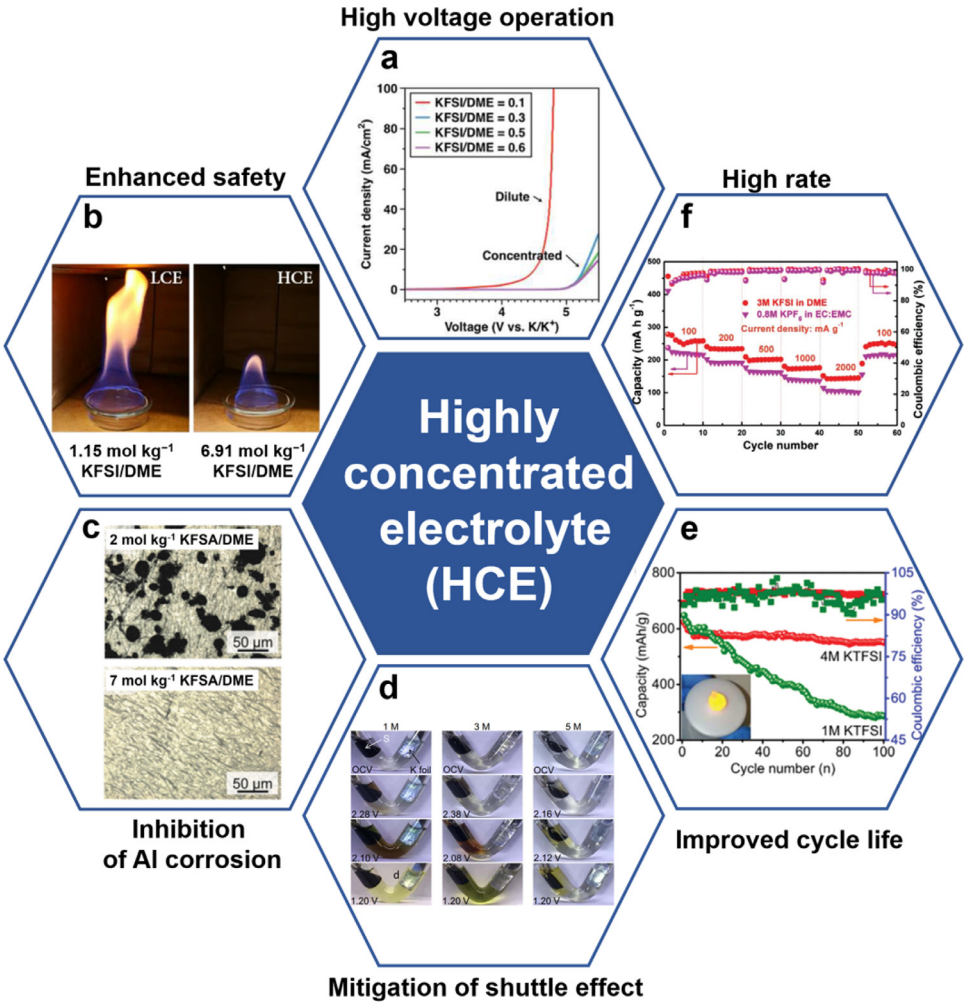

Figure 10. Advantages of concentrated electrolytes in KIB. (a) Electrochemical stability of different concentrations KFSI-DME electrolytes. Reproduced with permission [43]. Copyright 2017, American Chemical Society. (b) Flammability test of various concentrations electrolytes. Reproduced with permission [89]. Copyright 2019, Wiley-VCH. (c) Morphology of Al foil after cycles in different concentrations KFSI-DME electrolytes. Reproduced with permission [40]. Copyright 2018, The Royal Society of Chemistry. (d) Polysulfide shuttle behaviors in different concentrations KTFSI-DEGDME electrolytes. Reproduced with permission [90]. Copyright 2019, Elsevier B.V. (e) Cycling performance of Sb anode in different concentrations KTFSI-EC/DEC electrolytes. Reproduced with permission [91]. Copyright 2019, The Royal Society of Chemistry. (f) Rate capability of carbon anode in different concentrations electrolytes. Reproduced with permission [92]. Copyright 2018, Wiley-VCH.

The ideal electrolyte requires high ionic conductivity, low viscosity, no corrosion with the current collector, generation of a robust SEI on electrode surface, no decomposition at high and low potentials, inhibition some side reactions, and low cost, etc. If the above requirements cannot be met at the same time, a compromise can be made to maximize the performance of KIB.

3.2. Aqueous Electrolytes for KIB

The performance of aqueous KIB is mainly affected by K salt and concentration. Thus, recent advances in different K salts and concentrations for aqueous KIB will be discussed in detail as follows.

Typically, potassium nitrate (KNO_3), potassium sulfate (K_2SO_4), potassium acetate (KAc), KCF_3SO_3 or potassium hydroxide (KOH) are used as K salts and deionized water is used as solvent in aqueous KIB. Due to the active nature of K metal, platinum, Ag/AgCl, and activated carbon are usually used as counter electrodes in aqueous batteries. However, the hydrogen evolution potential and oxygen evolution potential limit the choice of electrode materials.

Cui *et al.* demonstrated insertion/extraction of K^+ in nickel hexacyanoferrate (NiHCF) in 1 M KNO_3-based electrolyte. **[**[93]**]** The study found that the reaction potential of K metal with NiHCF is 0.69 V. Besides, the battery shows a high capacity (59 mA h g^{-1} at C/6), high-rate capability (retention of 66% at 41.7 C) and stable cycling performance (a capacity decay rate of 0.00175%) due to the open framework structure and fast ionic diffusion of NiHCF in aqueous electrolyte (**Figure 11a**). Liu *et al.* reported aqueous KIB with Fe_3O_4-C anode and carbon nanotubes (CNTs) nanofilm cathode using 3 M KOH-based electrolyte. **[**[94]**]** The voltage curves present an obvious discharge platform at low current density, while it presents a linear state at high current density. The possible reason is the large difference in the rate capability of the cathode and anode in aqueous electrolyte (**Figure 11b**). $K_2Fe^{II}[Fe^{II}(CN)_6]\cdot 2H_2O$ nanocubes as aqueous KIB cathode demonstrated a discharge capacity of 120 mA h g^{-1} and long-term cycle life with a capacity retention of >85% over 500 cycles at 21.4 C in 0.5 M K_2SO_4-based electrolyte (**Figure 11c**) **[**[95]**]**.

In order to widen the electrochemical potential window of aqueous electrolytes, the $K(PTFSI)_{0.12}(TFSI)_{0.08}(OTf)_{0.8}\cdot 2H_2O$ hydrate melt with the lowest water content of 2.0 was discovered (**Figure 11d**) **[**[96]**]**. The salt benefits from the asymmetric imine anion ($PTFSI^-$), which provides low density, low viscosity, and low melting point in ILs. This enables the salt with good water solubility and is not affected by the S-F bond in water. Therefore, the electrochemical potential window of the K salt hydrate melt is significantly extended to 2.5 V. This is because all water molecules are coordinated with cations and hydrogen bonds are almost non-existent. Due to the use of asymmetric imine salts, the types of alkali metal hydrate melts have greatly increased, which will promote the development of electrolytes for safe high-voltage batteries.

In addition to the influence of K salts, electrolyte concentration affects ionic conductivity and rate ability of aqueous KIB. For example, the water-in-salt electrolyte (WiSE) has attracted widespread attention owing to the improved the electrochemical performance and enhanced safety of the battery. Ji *et al.* reported 30 M KAc-based WiSE used in aqueous KIB with a wide potential window of 3.2 V (**Figure 11e**). **[97]** The reversible redox behavior of $KTi_2(PO_4)_3$ anode in this electrolyte was achieved, avoiding the interference of a hydrogen evolution reac-

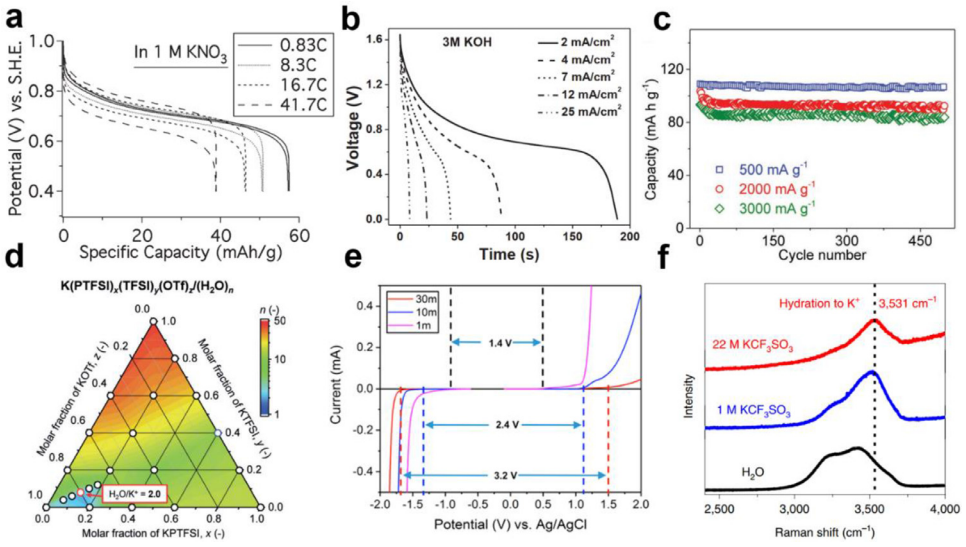

Figure 11. The electrochemical performance of various aqueous electrolytes. (a) Discharge curves of NiHCF in KNO_3-based electrolyte at various rates. Reproduced with permission [93]. Copyright 2011, American Chemical Society. (b) Voltage profiles of CNTs//Fe_3O_4-C in KOH-based electrolyte. Reproduced with permission [94]. Copyright 2015, Wiley-VCH. (c) Cycling performance of $K_2Fe^{II}[Fe^{II}(CN)_6]$•$2H_2O$ at different current densities in K_2SO_4-based electrolyte. Reproduced with permission [95]. Copyright 2017, Wiley-VCH. (d) Ternary phase diagram of $K(PTFSI)_x(TFSI)_y(OTf)_z$ salt. Reproduced with permission [96]. Copyright 2019, Wiley-VCH. (e) Linear sweep voltammetry profiles of KAc-based electrolytes with different concentrations. Reproduced with permission [97]. Copyright 2018, American Chemical Society. (f) Raman spectra of KOTf-based electrolytes with 1 M/22 M and H_2O. Reproduced with permission [98]. Copyright 2019, Springer Nature.

tion (HER) in dilute electrolyte. Besides, the ionic conductivity of KAc-based electrolyte is higher than LiTFSI-based electrolyte at the same concentration, which may attribute to the weak Lewis acidity of K^+, or the superiority of acetate salt. In addition, the polarization of 30 M KAc-based electrolyte is less than nonaqueous electrolytes. However, alkaline electrolytes are not compatible with many electrodes, which makes it important to develop compatible electrolytes. Recently, Hu *et al.* proposed a full aqueous KIB system using 22 M KCF_3SO_3-based electrolyte. **[98]** A high energy density of 80 Wh kg^{-1} and long-term cycling stability over 2000 cycles at 4 C are achieved in aqueous KIB, which are related to the highly concentrated KCF_3SO_3-based electrolyte with wide voltage window, high ionic conductivity, and low viscosity. Besides, it is found that the redox potential in 22 M electrolyte is lower than that in 1 M electrolyte due to the wide voltage window. In addition, high concentration electrolyte effectively suppresses the dissolution of 3, 4, 9, 10-perylenetetracarboxylic diimide (PTCDI) anode. This phenomenon was attributed to the domination of hydration K^+ in high concentration electrolytes, resulting that there are fewer freely moving water molecules (**Figure 11f**).

In summary, aqueous KIB has great application prospects in energy storage due to their high safety, low cost, and environmental friendliness. Nevertheless, aqueous batteries face a major problem that needs to be solved urgently, that is, lower battery voltage. **[99]** The narrow electrochemical window greatly limits the choice of electrode materials. Designing concentrated electrolytes can be considered as an effective strategy, but it will also greatly increase the cost of the battery. Therefore, the development of low-cost, high-stability aqueous electrolytes through some simple and effective strategies is extremely important for aqueous KIB.

3.3. Ionic Liquid Electrolytes for KIB

With reference to the research on IL electrolytes of LIB and SIB, it is found that IL electrolytes for KIB mainly focused on pyrrolidinamide (Pyr_{13}). Nohira *et al.* explored the chemical properties of KFSI-Pyr_{13}FSI IL for KIB. The ionic conductivity of 4.8 mS cm^{-1} was demonstrated when x(KFSI) is 0.20 at 298 K. **[44]** Besides, KFSI-Pyr_{13}FSI IL electrolyte exhibited a wider electrochemical window (5.72 V) than equivalent sodium (5.42 V) and lithium (5.48 V) ILs (**Figure 12a**). Recently, the application of KFSI-Pyr_{13}FSI IL in alloying materials (Sn_4P_3, Sn) for KIB was realized. **[51]** The cycling performance and battery safety have been effectively improved. A discharge capacity of 365 mA h g^{-1} over 100 cycles was achieved, which can be comparable to the rate capability in organic electrolytes of Sn_4P_3. The Sn anode exhibited a high capacity of over 170 mA h g^{-1} over 100 cycles due to the electrochemical stability of IL electrolyte (**Figure 12b**). **[100]** The P-type tetrathiafulvalene (Q-TTF-Q) delivered a higher capacity and a higher energy density with KFSI-Pyr_{13}FSI IL electrolyte than with conventional organic electrolyte (**Figure 12c**). **[101]** In addition, a potassium manganese hexacyanoferrate (KMF) cathode was demonstrated with a high working voltage (4.3 V to K/K^+) and a high CE of >99.3% in KFSI-based IL electrolyte. **[102]**

Apart from the FSI^- anion, $TFSI^-$ is also widely used in Pyr_{13}-based IL electrolytes. Masese *et al.* explored the electrochemical properties of KTFSI-Py_{r13}TFSI IL and revealed its redox voltage is lower than that of both Na and Li ILs. **[103]** A wide electrochemical window (~6.0 V) of KTFSI-based IL is exhibited, which is expected to endow KIB with high voltage and safety. Based on this IL electrolyte, stable cycling performance of layered cathode materials has achieved under high-voltage conditions. The average charge/discharge voltage of $K_2Ni_2TeO_6$ using 0.5 M KTFSI-Py_{r13}TFSI is 3.6 V versus K/K^+. Especially, P2-type $K_{2/3}Ni_{1/3}Co_{1/3}Te_{1/3}O_2$ with moderately inductive TeO_6^{6-} framework exhibits a record high voltage of 4.3 V versus K/K^+ (**Figure 12d**). **[104]** Additionally, $K_{2/3}Ni_{(2-x)/3}Co_{x/3}Te_{1/3}O_2$ (x=0.25, 0.5 and 0.75) is demonstrated to show good stability at 3.7 V, 3.85 V and 4.0 V, respectively. **[105]** However, the relatively low ionic conductivity and high viscosity at room temperature of this IL electrolyte hindered its further development.

In addition, the influence of cations and additives on electrode performance was studied in recent years. Balducci *et al.* investigated the physicochemical properties of pyrrolidinium-based aprotic IL (AIL-K) and protic IL (PIL-K) electrolytes with and without additive in hard carbon (HC) for KIB. **[106]** It is found that the ionic conductivity, viscosity, thermal stability, and electrochemical window of two IL electrolytes are comparable to those obtained for LIB and SIB. Besides, the reversible insertion/extraction of K^+ in HC can be realized in AIL-K electrolyte and hindered by the addition of VC (**Figure 12e**). In this regard, the VC in the electrolyte cannot contribute to the formation of a robust SEI. Furthermore, Pyr_{H4}TFSI electrolyte is electrochemically unstable, while Pyr_{14}TFSI electrolyte is stable at low potential. Otherwise, IL electrolyte (KTFSI-Pyr_{14}TFSI/ES) was used in K^+-based dual-graphite battery, which enables graphite anode with stable stability and a capacity of 230 mA h g^{-1}, and graphite cathode operation at 3.4-5.0 V vs. K/K^+. **[107]** Besides, the battery showed a high-capacity retention of 95% over 1500 cycles. ES additive is used to prevent Pyr_{14}^+ co-intercalation into graphite, which leads to the exfoliation of interlayer structure.

Currently, the influence of concentration on the performance of ILs has also attracted the attention of researchers. A K single cation IL (K-SCIL) as a highly concentrated electrolyte was developed by Matsumoto and coworkers to improve the K^+ transport (**Figure 12f**). **[108]** It is

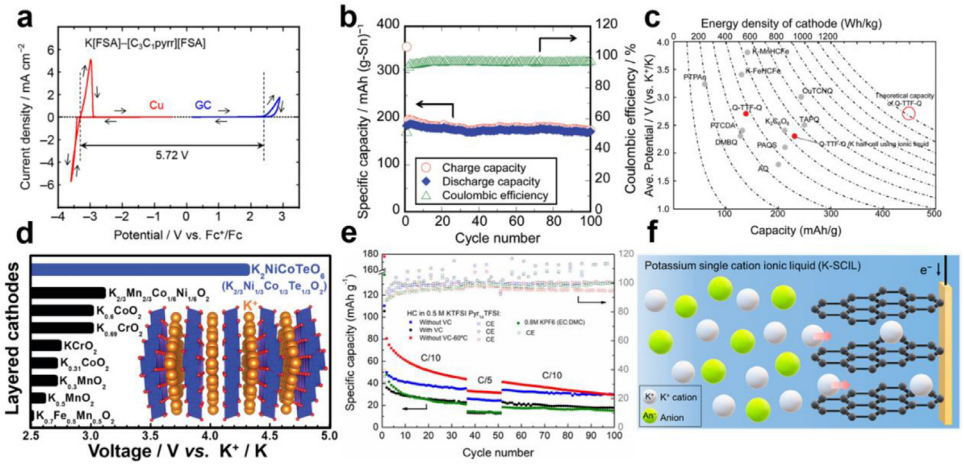

Figure 12. The electrochemical performance of various IL electrolytes. (a) CV of KFSI-Pyr_{13}FSI (x(KFSI) = 0.20) IL in a three-electrode cell. Reproduced with permission [44]. Copyright 2017, American Chemical Society. (b) Cycling performance of the Sn anode in KFSI-Pyr_{13}FSI IL electrolyte. Reproduced with permission [100]. Copyright 2020, The Royal Society of Chemistry. (c) Comparison of average voltage and capacity between Q-TTF-Q cathode using KFSI-Pyr_{13}FSI IL and the other organic cathodes. Reproduced with permission [101]. Copyright 2019, The Royal Society of Chemistry. (d) Comparison of the average voltage between P2-type $K_2NiCoTeO_6$ using KTFSI-Pyr_{13}TFSI IL and other layered cathodes. Reproduced with permission [104]. Copyright 2019, The Royal Society of Chemistry. (e) Cycling performance of HC in 0.5 M KTFSI-Pyr_{14}TFSI. Reproduced with permission [106]. Copyright 2019, Electrochemical Society, Inc. (f) Schematic illustration of a K single cation IL. Reproduced with permission [108]. Copyright 2020, American Chemical Society.

found that K^+ content is higher in K-SCIL electrolyte due to the absence of additional organic cation species. The low melting point (67°C) of K-$[FSI]_{0.55}[FTA]_{0.45}$ was obtained. They found the superconductivity of electrolyte under high temperature and large current, which is ascribed to the absence of K^+ concentration gradient. In addition, a wide electrochemical window of >5.0 V and good stability of graphite anode were realized in K-SCIL electrolyte.

Compared with the research of IL electrolytes in LIB and SIB, the research in KIB is still in its infancy. The wide voltage window of IL is the most outstanding property, indicating the significance of high voltage electrolytes. Nevertheless, higher viscosity, lower ion conductivity and high cost need to be further solved through various strategies. Regulating ionic salt chemistry may be an effective strategy. More types of anions (BF_4^-, $FeCl_4^-$) and cations (imidazolium, ammonium) combinations need to be developed. Further research on IL electrolytes will play a promising role in the development of high energy density KIB.

In a word, the electrochemical performance of the battery is closely related to the choice of electrolytes. Electrode materials show completely different specific capacities, cycling stability, CE, and rate capability in different electrolyte systems [89,109–127]. Therefore, engineering the electrolyte chemistry to promote the optimization of battery performance will be an important direction for the development of high-performance KIB in the future.

4. Solid Electrolyte Interfaces in KIB

The interface between electrode and electrolyte affects the electrochemistry of KIB, including SEI and CEI. Generally, the ideal interface in KIB is to allow K^+ to pass quickly and block the propagation of electrons. Until now, the understanding of interface in KIB is not as mature as the LIB/SIB, and it is in the initial stage. The fundamentals of SEI, including SEI formation mechanism, composition of SEI films, K^+ transport manners, influence factors of SEI in various electrodes, and interface engineering strategies for SEI, providing crucial guidance on the understanding and designing of SEI. In this section, the advances and perspectives in this field are comprehensively summarized and discussed.

4.1. The Formation Mechanism of SEI in KIB

It is well known that the dominant factors that affect the generation of the electrode/electrolyte interface are related to the behavior of initial surface specific adsorption and solvated coordination. The electric double layer (EDL) model was proposed by von Helmholtz and further optimized by Gouy-Chapman, and Stern. The probable scenarios of EDL are exhibited in **Figure 13a. [128]** The distribution of cations and anions with/without the diffusion layer on the charged/uncharged electrode are displayed. Besides, the compact layer and diffuse layer were explicitly recognized. It is found that the partial anions and small neutral molecules are adsorbed in the inner Helmholtz plane (IHP), while solvated molecules with large sizes are adsorbed in the outer Helmholtz plane (OHP) before cycling. Then, the SEI will be formed with the disappearance of specific absorption in EDL during cycling (**Figure 13b). [129,130]** The initial specific adsorption determines initial composition and structure of SEI. In addition, both the adsorbing side and the adsorbed side will affect the interface, include the properties of the electrode surface, the anions, cations, solvent molecules, and the spatial distribution of the adsorption layer, etc.

Solvated coordinate structure is another important factor that affects SEI. In fact, the solvated coordinate structure is derived from the interaction between electrolyte solvents and K^+. Typically, solvation structures, coordination numbers, and desolvation energy of K^+ with 27 organic solvents are investigated. **[18]** It is found that the K^+ complexes exhibit lower desolvation energy than Li^+, Na^+, and Mg^{2+}. At the same time, the solvation behaviors are affected by salt, solvent, additive, and concentration. Notably, higher solvation energy of KFSI-based electrolyte compared to KPF_6-based electrolyte makes the side reaction greatly reduced (**Figure 13c). [53]** Then, the solvation energy of EC/DEC-based system is lower than that of DME-based system, indicating the rapid diffusion of K^+ and convenience of desolvation. Moreover, the solvation energy of the electrolyte is increased due to the presence of additives, making K^+ diffusion and desolvation more difficult (**Figure 13d). [50]** This result also reveals the reason why the electrochemical performance of the GeP_5 electrodes deteriorates with additives.

Additionally, the solvation of K^+ with both FSI^- and TEP increases and free solvent molecules decrease as the electrolyte concentration increases. **[46]** The solvation ratio of K^+/TEP is much lower than that of Na^+/TMP and Li^+/TEP at a similar concentration, indicating the weaker solvation of K^+ than Li^+ and Na^+. Besides, the low viscosity and high ionic conductivity of K^+/TEP is consistent with the low solvation ratio (**Figure 13e**). In addition, free DME, free FSI^-, and solvated K^+ are in low concentration electrolyte, while the contact ion pairs and aggregate species are in high concentration electrolyte. Meanwhile, localized high-concentration electrolyte (LHCE) with a highly fluorinated ether (HFE) maintain the local coordination structure of cations. **[89]** The reinforced 3D network is broken, thus resolving poor wettability of HCE (**Figure 13f**).

Recently, Ming *et al.* analyzed the reaction pathway for the purpose of better understand the cation-solvent structure on the metal electrode. **[131]** They found that the behavior of K^+-solvent structure accepting

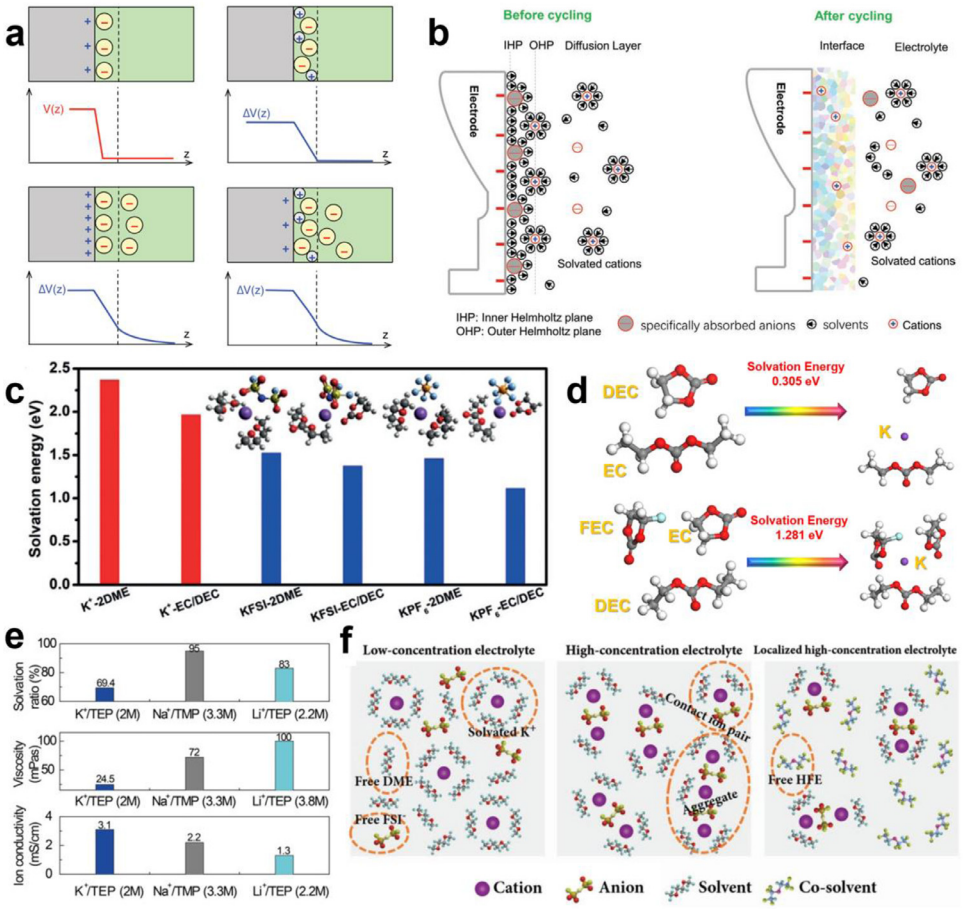

Figure 13. The initial surface specific adsorption behaviors and solvated coordination behaviors. (a) Schematic diagram of possible situation for electric double layers. Reproduced with permission [128]. Copyright 2019, Elsevier B.V. (b) Schematic diagram of the specific absorption before and after cycling. Reproduced with permission [129]. Copyright 2009, The Royal Society of Chemistry. (c) Solvation energies of solvated K^+ and K salt-solvent complexes in EC/DEC and DME-based electrolytes. Reproduced with permission [53]. Copyright 2019, Wiley-VCH. (d) Solvation energies estimated of EC/DEC-based electrolytes with/without FEC. Reproduced with permission [50]. Copyright 2018, Elsevier B.V. (e) Comparison of solvated solvent ratio, viscosity, and ionic conductivity in KFSI, NaFSI, and LiFSI-based electrolytes. Reproduced with permission [46]. Copyright 2020, Wiley-VCH. (f) Solution structures of low concentration, high concentration, and localized high concentration electrolytes. Reproduced with permission [89]. Copyright 2019, Wiley-VCH.

an electron can induce the decomposition of electrolyte. Besides, the adjustment of electronegativity through changing the anion type, solvent chemistry and concentration can effectively inhibit the decomposition of electrolyte.

4.2. The Composition of SEI in Various Electrodes

In general, the structure of SEI is a complex layer, including organic components and inorganic components. The representative organic components are RO-COOK and RO-K (R = alkyl groups), while the typical inorganic compounds are detected to be KF, K_2CO_3, $KHCO_3$, K_2O, KPF_6, KFSI, K_2S, KSON, K_2SO_4, K_2SO_3, $K_2S_2O_3$, R-S, $KHSO_4$, F_2S, S, P, phosphates, N-containing products, etc. **[46,66,67,88,92,132]** These products vary with the potential and depth of electrodes. The organic components of SEI are mainly formed by the decomposition of organic solvents and the deposition of K-containing species. For example, the bonding of C–O, C=O, and O–C=O originates from the decomposition products of solvents (EC, DEC, EMC, PC, DME, FEC). The inorganic KF in the SEI originates from the reactions between F^- (degeneration of KPF_6 or KFSI, the decomposition of FEC additives, or polyvinylidene fluoride (PVDF)) and K^+. For an instance, the P-F bonds are observed in KPF_6-based electrolytes. The S-based component ($-SO_xF$, $-SO_2F$, $-SO_2-$, S=O, S^0 and K_xS_y species) and N-containing products are derived from the decomposition products of KFSI salt. The S-F bonds should be related to the decomposition products of KFSI. The P element is possible from TEP solvent.

4.3. Influence Factors on SEI in Various Electrodes

The research on SEI layer is mainly based on different electrodes, and different electrolyte compositions and concentrations. Hence, the detailed investigation of SEI formed on different electrodes are introduced. The connection between the material and generated SEI should be established, and better electrochemical performance can be obtained by optimizing the electrolyte composition or concentration.

4.3.1. SEI in Carbon-Based Materials

Graphite as a KIB anode is considered a prospective candidate due to its high ionic conductivity and abundant natural resource. However, the K storage performance and mechanism of graphite anode are closely related to SEI, which plays a critical role in ensuring the reversibility and stability of battery.

Effect of salts on SEI. The SEI film in KPF_6-based electrolyte is thick, rough, and ruptured, while the SEI in KFSI-based electrolyte exhibits a thin, smooth, and intact film. **[57]** It is found that anions (PF_6^- and $KFSI^-$) and K^+ are likely to co-intercalate into the graphite during the SEI formation process. Nevertheless, it is easier for PF_6^- ions to intercalate into the graphite layers due to its smaller size. Thus, the graphite layers are damaged, causing the continuous electrolyte decomposition and repairing the damaged SEI. In contrast, $KFSI^-$ ions are difficult to insert into the graphite layers with large size and the strong interaction between graphite and $KFSI^-$ ions, realizing the formation of stable and uniform SEI layers (**Figure 14a**).

Effect of solvents on SEI. It is found that the electrochemical behaviors of graphite vary with different solvents (such as carbonate-based and ether-based solvents). Kang group systematically studied the effect of graphite SEI on capacity attenuation in EC/DEC and DEGDME-based electrolytes. **[112]** One of the reasons on capacity decay is that the decomposition of EC/DEC-based electrolyte causes the SEI growth to become thicker, while the DEGDME-based electrolyte is relatively stable. Thus, the SEI on K anode is more stable in DEGDME than in EC/DEC. Subsequently, the electrochemical behaviors of graphite an-

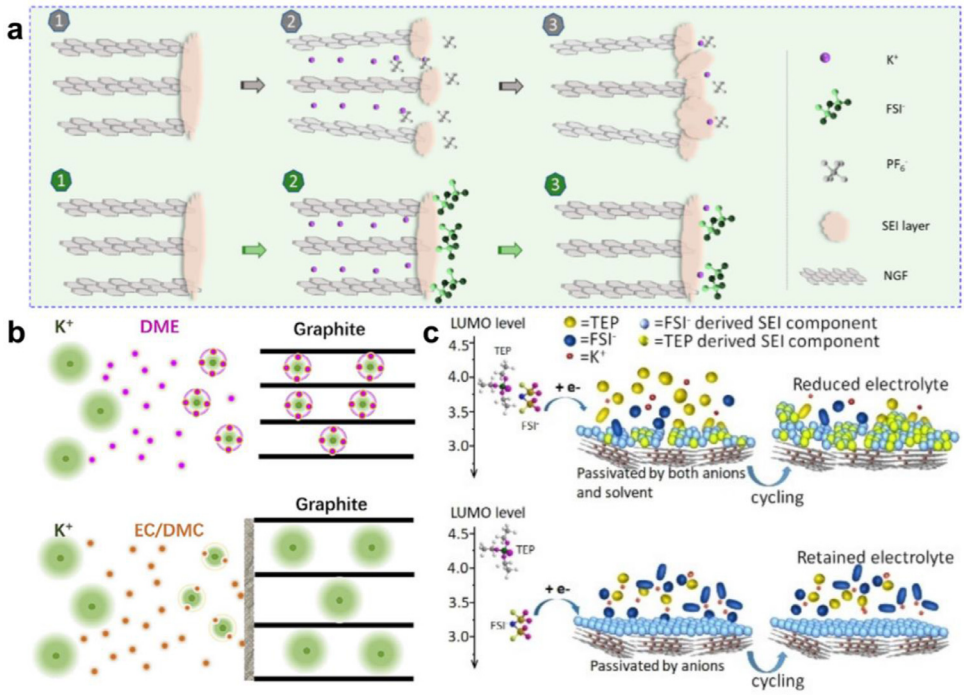

Figure 14. The SEI in carbon electrodes. Schematic illustration of SEI formation on graphite anode in (a) KPF_6 and KFSI-based electrolytes. Reproduced with permission [57]. Copyright 2019, American Chemical Society. Schematic illustration of SEI formation on graphite anode in (b) DME and EC/DMC-based electrolytes. Reproduced with permission [65]. Copyright 2019, Elsevier B.V. Schematic illustration of SEI formation on graphite anode in (c) 0.9 M KFSI and 2.0 M KFSI-based electrolytes. Reproduced with permission [46]. Copyright 2020, Wiley-VCH.

ode in EC/DMC and DME-based electrolytes were also investigated. **[65]** A high ICE of 87% is achieved in DME-based electrolytes, which is ascribed to the almost no formation of SEI. Besides, the discharge voltage in DME system is much higher than in EC/DMC one, which is attributed to the formation of $[K\text{-}DME_y]^+$-graphite complex. Therefore, the $[K\text{-}DME_y]^+$ complex co-intercalating into graphite leads to outstanding rate performance, a negligible SEI film, and a small volume expansion (**Figure 14b**). Recently, the K^+-solvent co-intercalation mechanism of graphite anode in DEGDME-based electrolyte was furtherly confirmed. **[73]** The solvation energy, desolvation energy, LUMO levels of $[K\text{-solvent}]^+$ complexes are compared, and the Fermi level of graphite are calculated. It is found that the $[K\text{-DEGDME}]^+$ complexes with strong solvation and higher LUMO levels are suitable for reversible co-intercalation. Moreover, the thermodynamic and chemical stability of $[K\text{-DEGDME}]^+$ complexes are superior. In addition, the graphite with fast kinetics is due to the avoidance of sluggish desolvation process for $[K\text{-DEGDME}]^+$ complexes.

Effect of concentrations on SEI. The SEI formation mechanism of graphite in different concentrations electrolyte is revealed. **[46]** The LUMO level of the FSI^- anions and TEP is located at around 3.5 eV in diluted electrolyte, while it is totally occupied by FSI^- in concentrated electrolyte. Thus, the SEI formation of graphite in 0.9 M KFSI-based electrolyte is involved to the decomposition of solvent and anions, leading to the formation of uneven and unstable SEI. In contrast, $KFSI^-$ ions dominate in the formation of SEI and the solvent decomposition is effectively suppressed in 2 M KFSI- based electrolyte, promoting the generation of uniform and stable SEI (**Figure 14c**). Especially, the ultra-thin SEI film with less than 1.0 nm thickness on graphite surface is realized in a LHCE. Besides, The KF-rich SEI film is durable, preventing the co-intercalation of solvated K^+ into interlayer, thus maintaining the layered structure of pristine graphite.

4.3.2. SEI in Alloy-Based Anodes

The alloy anodes (Sb, SnSb, Sn_4P_3, P, and Bi) deliver high K storage capacity. Nonetheless, the poor rate capability and fast capacity decay hamper their application owing to the slow kinetics and huge volume expansion. Thus, it is essential here to build a robust SEI on alloy anodes, constructing structural stability of alloy anodes toward long-cycle life.

Effect of salts on SEI. The SEI film formed in KFSI-based electrolyte is uniform and stable. **[49]** The ruptured SEI film on the surface of Bi/rGO anode was discovered in KPF_6-based electrolyte, which is attributed to the huge volume expansion of the Bi nanoparticles. The crevices of SEI will lead to the further decomposition of the electrolyte. By contrast, the integrity of SEI film was maintained in KFSI-based electrolyte, which could suppress the continuous side reactions on the interface of the electrolyte/electrode (**Figure 15a and b**). In addition, the cycling performance of RP/C anode for KIB in KFSI-based electrolyte are superior to the other electrolytes, indicating more stable formed SEI film on the electrode in KFSI-based electrolyte during cycling. **[53]**

Effect of solvents on SEI. The SEI formed on the electrode surface in DME is thinner than that in EC/DEC. For an instance, the Nyquist plots of SnSb anode after cycles showed a negligible SEI film impedance in DME-based electrolyte and an obvious SEI impedance in EC/DEC-based electrolyte (**Figure 15c and d**). **[70]** This result shows that DME-based electrolyte decomposes relatively little, forming a relatively thin SEI, thus improving the ICE of the electrode. Besides, the elastic and continuous SEI layer was found on the surface of Bi anode in DME-based electrolyte, strongly keeping particles integrated to avoid the loss of active material. **[113]** With the protection of SEI, the fragments of microparticles did not generate more fresh electrode/electrolyte interfaces. In contrast, the much severe pulverization and visible electrode isolations of Bi anode after cycles in EC/PC-based electrolytes were found.

Effect of additives on SEI. The FEC promotes the formation of inhomogeneous SEI film. To investigate the effect of FEC in the SEI formation, the morphology of Sn_4P_3 electrode surface after cycles was observed. **[51]** It is found that Sn_4P_3 anode exhibited a smooth surface in electrolytes without FEC, while small particles can be discovered on the surface of Sn_4P_3 anode in electrolytes with FEC (**Figure 15e-h**). Further research proves that the element tin content of the particles is significantly higher than other regions, indicating that the SEI with FEC is not uniform.

Effect of concentrations on SEI. In addition, the effect of dilute and concentrated electrolytes on the SEI formation of Sb@carbon sphere network (CSN) is different. **[91]** Obviously, anions ($TFSI^-$ ions) with faster kinetic are much easier to diffuse to the interface and participate in the formation of SEI in a high-concentration electrolyte. The concentrated

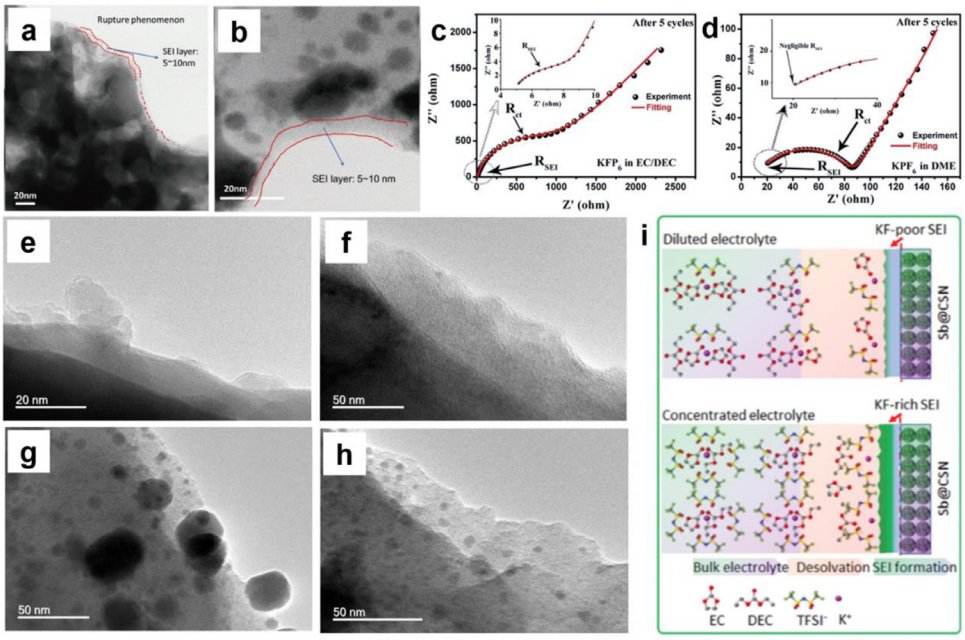

Figure 15. The SEI in alloy-based electrodes. TEM images of Bi@rGO anode after five cycles in (a) KPF_6 and (b) KFSI-based electrolytes. Reproduced with permission [49]. Copyright 2018, Wiley-VCH. Electrochemical impedance spectra of SnSb anode in (c) EC/DEC and (d) DME-based electrolytes after 5 cycles. Reproduced with permission [70]. Copyright 2019, The Royal Society of Chemistry. TEM images of Sn_4P_3 anode after 350 cycles in (e) KPF_6-EC/DEC, (f) KFSI-EC/DEC, (g) KPF_6-EC/DEC/FEC (5 wt%), (h) KFSI-EC/DEC/FEC (5 wt%) electrolytes. Reproduced with permission [51]. Copyright 2019, Electrochemical Society of Japan. (i) Illustration of the SEI layer formation on Sb@CSN anode in 1.0 M KTFSI-based and 4.0 M KTFSI-based electrolytes. Reproduced with permission [91]. Copyright 2019, The Royal Society of Chemistry.

K^+ promotes a thinner and denser SEI layer with KF-rich preferentially formed in concentrated electrolyte (**Figure 15i**).

4.3.3. SEI in Metal Sulfide Anodes

Transition metal sulfides (TMSs) are attractive anodes for KIB due to their high capacities, abundant resource, and environment friendliness. However, the problem of volume expansion during charging/discharging is still serious. Thus, stable SEI that reducing the interface impedance, thereby extending battery cycle life is needed.

The SEI of $NiCo_{2.5}S_4$@reduced graphene oxide (NCS@RGO) anode formed in KFSI-EC/PC electrolyte is the thinnest compared with other electrolytes. **[55]** It is found that the thicknesses of SEI layers on electrodes using KFSI-EC/PC, KFSI-EC/PC/FEC, KPF_6-EC/PC, and KPF_6-EC/PC/FEC electrolytes are about 7, 46, 53, and 23 nm, respectively (**Figure 16a-d**). It shows that the SEI layer formed in the KFSI-EC/PC electrolyte is the most uniform and dense, which is expected to achieve rapid K^+ transport. Only needlelike dendrites in the electrodes did not appear in the KFSI-EC/PC electrolyte, indicating that stable SEI effectively prevents the side reaction between the electrolyte and K metal.

The effect of K salt on the electrochemical performance of MoS_2 anode was investigated. **[54]** It is found that the CE and capacity retention of MoS_2 anode using KFSI-based electrolyte are much higher than those in KPF_6-based electrolyte. The SEI film formed in KFSI-based electrolyte is stable and KF-rich, while SEI film in KPF_6-based electrolyte is unstable, KF-deficient, and organic species-rich (**Figure 16e**).

The concentration of electrolyte affects the thickness and composition of SEI. **[121]** As schematic illustrations of SEI formed in different concentration electrolytes, the thick and uniform SEI film is formed in 1 M KFSI-based electrolyte, while the thinner and uniform SEI film is formed in 4 M KFSI-based electrolyte (**Figure 16f**). The SEI in dilute electrolyte may from the solvent reduction, while the SEI in concentrated electrolyte may from the salt reduction.

4.3.4. SEI in Organic Electrodes

Organic electrodes have attracted wide attention in KIB owing to their renewability, low cost, environment-friendly, and better safety. However, since organic materials are easily soluble in organic electrolytes, the presence of SEI is particularly important.

The ether-based electrolytes promote the generation of compact and stable SEI layer. Hence, the effect of solvents on the generation of SEI film on anthraquinone-1, 5- disulfonic acid sodium salt (AQDS) cathodes in KIB was explored. **[66]** It is found that the thickness of SEI films in DME and EC/DEC-based electrolytes are about 5 nm and 10 nm, respectively. In DME-based electrolyte, the FSI^- is preferentially decomposed and then the solvent molecule is decomposed during the formation of SEI due to the big LUMO energy level difference between FSI^- and DME molecules. Thus, the formed SEI layer is inorganic-rich, which could effectively mitigate the decomposition of DME-based electrolyte (**Figure 17a**). In contrast, possible simultaneous decomposition of FSI^-, EC, and DEC occurs due to the highly close LUMO energy levels among them in EC/DEC-based electrolyte. Thus, the formed SEI film is inorganic distributed randomly, which is tends to fracture more easily after cycles (**Figure 17b**).

The SEI film plays a critical role in the cycling performance of K_2TP electrode. **[67]** It is found that the electrochemical stability of K_2TP in DME-based electrolyte is most excellent. The SEI film formed in DME-based electrolytes is thinner than that in carbonate electrolytes (**Figure 17c and d**). Besides, the charge transfer resistance in DME-based electrolyte is one order of magnitude less than that in carbonate electrolytes. In addition, the formed SEI film in DME-based electrolyte is highly K^+-conductive and robust.

4.4. Interface Engineering Strategies for SEI

Interface engineering can effectively strengthen the properties of SEI, and then achieve the purpose of optimizing electrochemical performance. For an instance, an artificial SEI layer or preformed passivation layer have been applied successfully in KIB. Ultra-smooth and ultra-thin SEI films on K metal surfaces were realized by electrochemical polishing [133]. Generally, the microscopic protrusion is one of detriment factors that promote dendrite growth of K metal anode. The rough morphology promotes the growth of K dendrites and the formation of uneven and unstable SEI, while the smooth morphology realized the formation of stable and uniform SEI without the growth of dendrites (Figure 18a). In this way, the cycling stability at least 200 cycles (0.02 mA h cm^{-2} at 0.1 mA cm^{-2}) of polished K metal anodes is significantly enhanced (Figure 18b).

A CNT coating layer is a kind of promising artificial SEI design, which is suitable for K metal [134]. A strong interfacial interaction between the CNT and K metal anode avoids uneven electrodeposition of K^+. The

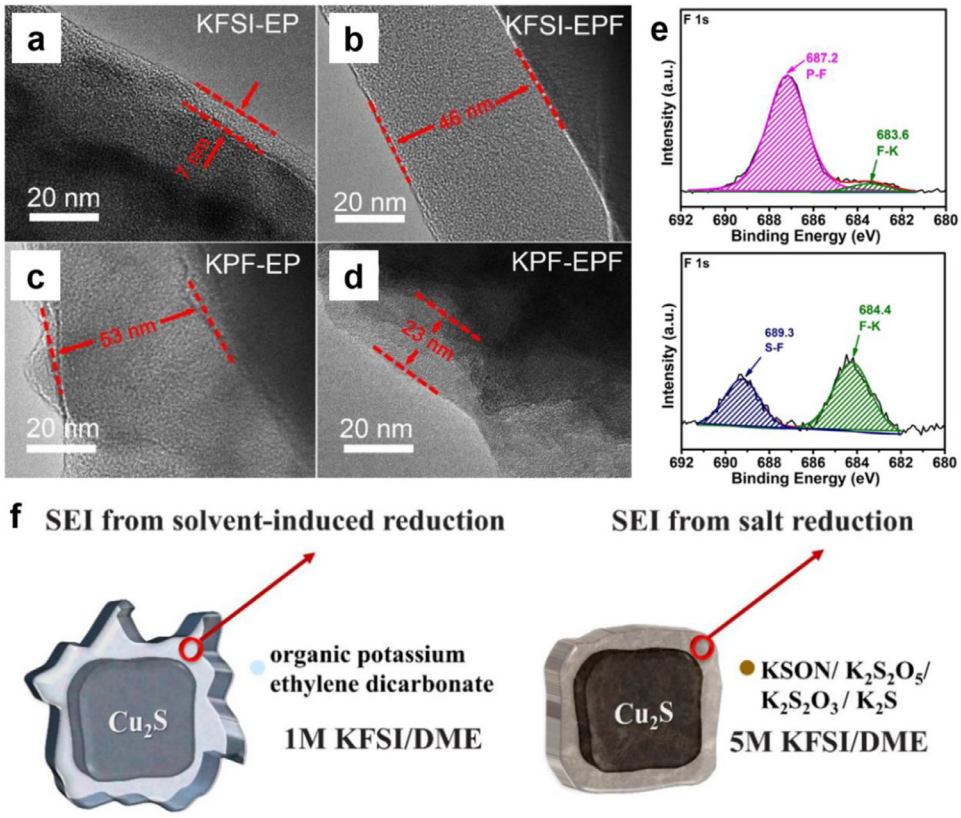

Figure 16. The SEI in metal sulfide electrodes. TEM images of NCS@RGO anode in (a) KFSI-EC/PC, (b) KFSI-EC/PC/FEC (5 wt%), (c) KPF_6-EC/PC and (d) KPF_6-EC/PC/FEC (5 wt%) electrolytes after 50 cycles. Reproduced with permission [55]. Copyright 2019, Wiley-VCH. (e) Comparison of F 1s X-ray photoelectron spectroscopy (XPS) spectra on MoS_2 anode in KPF_6 and KFSI-based electrolytes. Reproduced with permission [54]. Copyright 2019, American Chemical Society. (f) Illustration of SEI formation on Cu_2S anode in 1 M KFSI and 5 M KFSI-based electrolytes. Reproduced with permission [121]. Copyright 2020, American Chemical Society.

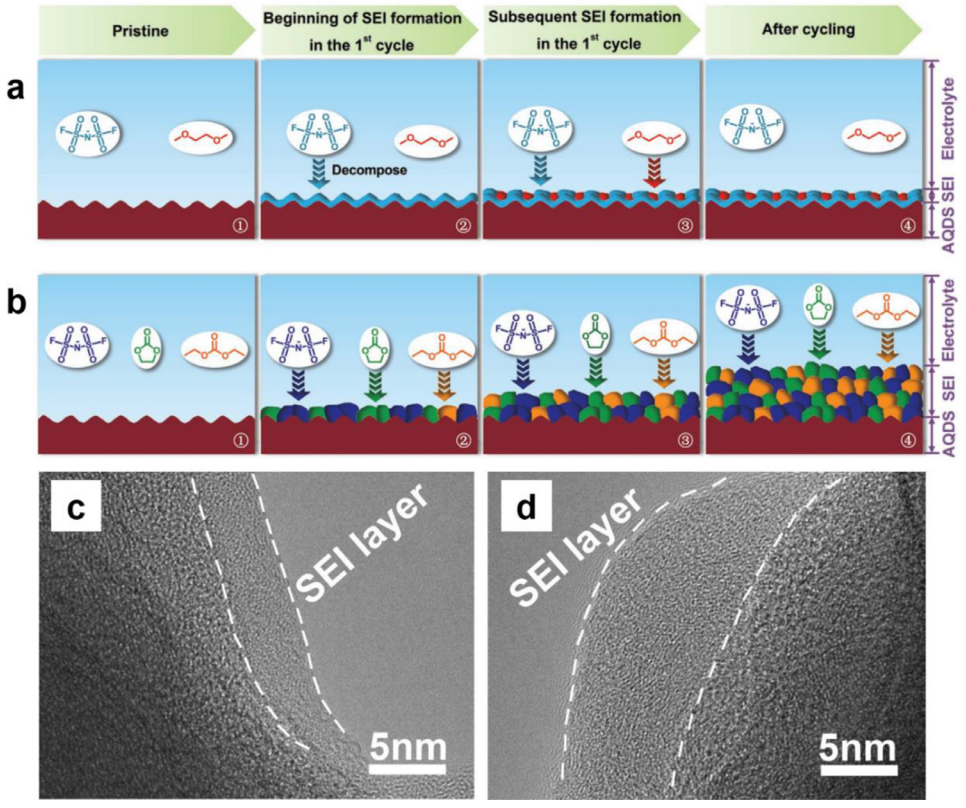

Figure 17. The SEI in organic electrodes. Schematic illustration of the SEI formation on AQDS cathode in (a) DME and (b) EC/DEC-based electrolytes. Reproduced with permission [66]. Copyright 2018, Wiley-VCH. HRTEM images of K_2TP anode in (c) DME and (d) PC-based electrolytes after cycles. Reproduced with permission [67]. Copyright 2017, The Royal Society of Chemistry.

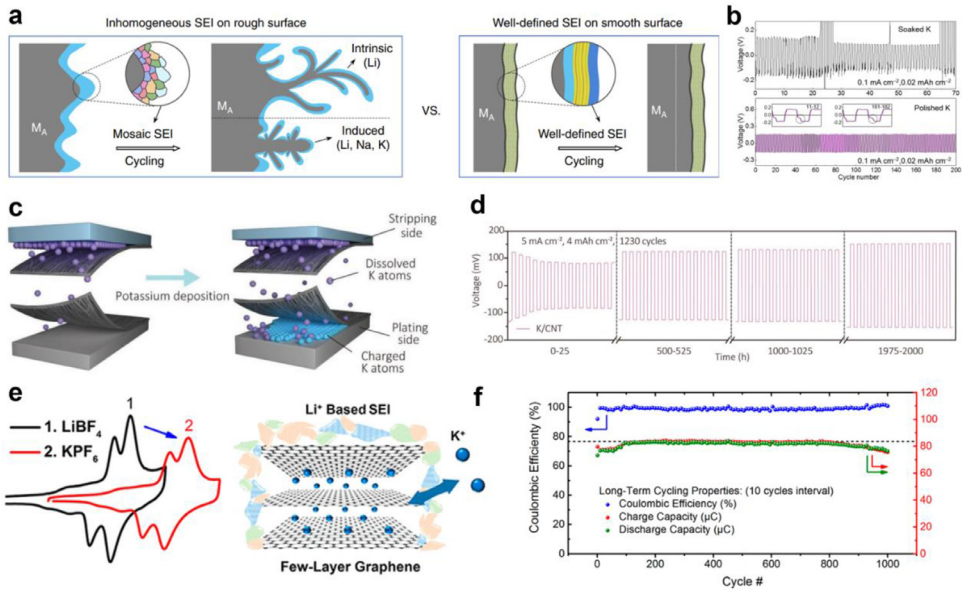

Figure 18. Artificial SEI Design in KIB. (a) Illustration of SEI formation on a rough surface and a smooth surface during cycling process. (b) Cycling performance of polished and soaked K anodes. Reproduced with permission [133]. Copyright 2018, Springer Nature. (c) Schematic illustration of K plating within the K/CNT. (d) Cycling stability of the K/CNT. Reproduced with permission [134]. Copyright 2019, Wiley-VCH. (e) CV tests of graphene which initially in Li^+ containing electrolyte then in K^+ containing electrolyte and schematic illustration of the K^+ insertion/extraction in graphite layers with the Li^+-based SEI. (f) Long-term cycling of the graphene. Reproduced with permission [135]. Copyright 2018, American Chemical Society.

CNT serves as a hosting medium for regulating the stripping/plating behavior of K^+. A robust and uniform SEI was formed spontaneously on the CNT surface (Figure 18c). Notably, a deposition amount of 20 mA h cm^{-2} was achieved with the artificial SEI of CNT. Besides, long-term cycling lifespan over 1000 cycles and an areal capacity of 4 mA h cm^{-2} were obtained even at 5 mA cm^{-2} (Figure 18d).

In addition, Li^+-based SEI promote the efficient and fast K^+ intercalation on graphene electrode [135]. First, graphene is pretreated in a $LiBF_4$ electrolyte to form a Li-containing SEI layer. Then, the intercalation peaks of K^+ were well-defined. It is found that the characteristics of the intercalation peaks of Li^+ and K^+ are very similar, indicating a comparable staging-type intercalation process (Figure 18e). The reversible intercalation behavior of K^+ is attributed to the pretreated Li^+-based SEI on the graphene. As a result, stable long-term cycle life (1000 cycles) and high-rate capability (~360 C) of graphene electrode are achieved (Figure 18f).

The strategy adopted for LIB/SIB can be applied to KIB, but the interface behaviors among the three battery systems are very different. More improvement strategies belonging to KIB need to be explored. Although the research on artificial SEI is still in its infancy, the artificial SEI method is a supplement to electrolyte optimization and has a promoting effect on the development of high-performance KIB.

5. Conclusion and Future Directions

In summary, the development of high-performance KIB should give priority to the development of electrolytes and interfaces. The solvation structure can be adjusted by regulating the salt, solvent, additives, and concentration to establish the interface compatibility of the electrolyte system. By studying and understanding the formation mechanism, composition, influencing factors and improvement strategies of SEI of different materials in different electrolyte systems, we can design and realize better performance KIB electrolytes. Finally, we outline potential directions and future prospects for KIB electrolytes and hope that our perspectives may be helpful for the development of high-performance KIB.

(1) The design of advanced electrolytes. In the case of organic electrolytes, a suitable electrolyte can not only form a stable SEI on the anode surface, but also stabilize the cathode materials at high voltage. (i) The electrolytes for advanced K-ion full batteries may be important research direction in the future. (ii) The electrolytes can operate in a wide temperature range. The development of more chemically stable solvents or additives can achieve this requirement. (iii) The development and design of new additives can simultaneously achieve high CE and long cycling life. For aqueous electrolytes, it is urgent to develop effective strategies to expand the electrochemical potential window and avoid decomposition of water and electrolytes. Adjusting and optimizing the electrolyte formulation may solve the above problems. In addition, reducing the cost of IL electrolytes is the focus of future researches. It is possible to mix IL with other electrolytes to reduce costs while maintaining the original properties. As for solid electrolytes, the nanostructure design of solid electrolytes can be an effective strategy to improve ionic conductivity. Constructing an anion framework to increase the distance between anions and cations is expect to enhance the transport of ions. Additionally, building a hybrid electrolyte that meets various needs will be a meaningful exploration.

(2) The further investigations on developing strategies to stabilize the electrode/electrolyte interface upon repeated K^+ insertion/extraction. Electrolyte optimization is an efficient strategy to solve the side reactions at the interface in KIB. Besides, the artificial SEI can effectively prevent the contact of active K with the electrolytes, so it may fundamentally solve the challenge of SEI instability.

(3) The development of advanced characterization techniques (such as *in situ* Raman spectroscopy, Fourier transform infrared microscopy (FTIR), nuclear magnetic resonance (NMR), and cryo-electron microscopy, etc.) and theoretical simulation (Molecular Dynamic simulation) can understand the electrolyte structure and chemistry (K^+ solvation, transport pathway of K^+, the formation and evolution of SEI).

Overall, the KIB technology is becoming a very competitive candidate for large-scale energy storage systems. Electrolyte and electrolyte/electrode interface are the top priority for the development of high-performance KIB. Therefore, it is very vital to provide a comprehensive summary for the research of KIB electrolytes and SEI to make KIBs feasible in the near future.

Declaration of Competing Interest

The authors declare they have no known competing financial interests or personal relationships that could have appeared to influence the work reported in this paper.

Acknowledgements

This work was supported by the National Natural Science Foundation of China (51832004, 21905218), the National Key Research and Development Program of China (2020YFA0715000), the Natural Science Foundation of Hubei Province (2019CFA001, 2020CFB519), the Foshan Xianhu Laboratory of the Advanced Energy Science and Technology Guangdong Laboratory (XHT2020-003), Sanya Science and Education Innovation Park of Wuhan University of Technology (2020KF0019), and the Fundamental Research Funds for the Central Universities (WUT: 2020IVB034, 2020IVA036).

References

[1] B. Dunn, H. Kamath, J.M. Tarascon, Electrical Energy Storage for the Grid: A Battery of Choices, Science 334 (2011) 928–935.
[2] M.M. Thackeray, C. Wolverton, E.D. Isaacs, Electrical energy storage for transportation-approaching the limits of, and going beyond, lithium-ion batteries, Energy Environ. Sci. 5 (2012) 7854–7863.
[3] D. Larcher, J.M. Tarascon, Towards greener and more sustainable batteries for electrical energy storage, Nat. Chem. 7 (2015) 19–29.
[4] J.M. Tarascon, M. Armand, Issues and challenges facing rechargeable lithium batteries, Nature 414 (2001) 359–367.
[5] E.A. Olivetti, et al., Lithium-Ion Battery Supply Chain Considerations: Analysis of Potential Bottlenecks in Critical Metals, Joule 1 (2017) 229–243.
[6] A. Eftekhari, Z. Jian, X. Ji, Potassium Secondary Batteries, ACS Appl. Mater. Interfaces 9 (2017) 4404–4419.
[7] K. Kubota, et al., Towards K-Ion and Na-Ion Batteries as “Beyond Li-Ion”, Chem. Rec. 18 (2018) 459–479.
[8] A. Eftekhari, Potassium secondary cell based on Prussian blue cathode, J. Power Sources 126 (2004) 221–228.
[9] Z. Xiao, et al., K^+ modulated K^+/vacancy disordered layered oxide for high-rate and high-capacity potassium-ion batteries, Energy Environ. Sci. 13 (2020) 3129–3137.
[10] T. Hosaka, et al., Research Development on K-Ion Batteries, Chem. Rev. 120 (2020) 6358–6466.
[11] X. Wu, D.P. Leonard, X. Ji, Emerging Non-Aqueous Potassium-Ion Batteries: Challenges and Opportunities, Chem. Mater. 29 (2017) 5031–5042.
[12] J.C. Pramudita, et al., An Initial Review of the Status of Electrode Materials for Potassium-Ion Batteries, Adv. Energy Mater. 7 (2017) 1602911.
[13] J.-Y. Hwang, S.-T. Myung, Y.-K. Sun, Recent Progress in Rechargeable Potassium Batteries, Adv. Funct. Mater. 28 (2018) 1802938.
[14] Y. Huang, et al., Electrolytes and Electrolyte/Electrode Interfaces in Sodium-Ion Batteries: From Scientific Research to Practical Application, Adv. Mater. 31 (2019) 1808393.
[15] C. Bommier, X. Ji, Electrolytes, SEI Formation, and Binders: A Review of Nonelectrode Factors for Sodium-Ion Battery Anodes, Small 14 (2018) 1703576.
[16] S. Komaba, et al., Potassium intercalation into graphite to realize high-voltage/high-power potassium-ion batteries and potassium-ion capacitors, Electrochem. Commun. 60 (2015) 172–175.
[17] N. Matsuura, K. Umemoto, Z.i. Takeuchi, Standard Potentials of Alkali Metals, Silver, and Thallium Metal/Ion Couples in N, N′-Dimethylformamide, Dimethyl Sulfoxide, and Propylene Carbonate, Bull. Chem. Soc. Jpn. 47 (1974) 813–817.
[18] M. Okoshi, et al., Theoretical Analysis of Interactions between Potassium Ions and Organic Electrolyte Solvents: A Comparison with Lithium, Sodium, and Magnesium Ions, J. Electrochem. Soc. 164 (2017) A54–A60.
[19] X. Wang, et al., Earth Abundant Fe/Mn-Based Layered Oxide Interconnected Nanowires for Advanced K-Ion Full Batteries, Nano Lett. 17 (2017) 544–550.
[20] M. Huang, et al., Ultra-fast and high-stable near-pseudocapacitance intercalation cathode for aqueous potassium-ion storage, Nano Energy 77 (2020) 105069.
[21] X. Wang, et al., Polycrystalline soft carbon semi-hollow microrods as anode for advanced K-ion full batteries, Nanoscale 9 (2017) 18216–18222.
[22] K. Han, et al., Three-dimensional carbon network confined antimony nanoparticle anodes for high-capacity K-ion batteries, Nanoscale 10 (2018) 6820–6826.
[23] X. Wang, et al., Graphene oxide-wrapped dipotassium terephthalate hollow microrods for enhanced potassium storage, Chem. Commun. 54 (2018) 11029–11032.
[24] H. Che, et al., Electrolyte design strategies and research progress for room-temperature sodium-ion batteries, Energy Environ. Sci. 10 (2017) 1075–1101.
[25] G.G. Eshetu, et al., Electrolytes and Interphases in Sodium-Based Rechargeable Batteries: Recent Advances and Perspectives, Adv. Energy Mater. 10 (2020) 2000093.
[26] M. Li, et al., New Concepts in Electrolytes, Chem. Rev. 120 (2020) 6783–6819.
[27] K. Xu, Electrolytes and Interphases in Li-Ion Batteries and Beyond, Chem. Rev. 114 (2014) 11503–11618.
[28] M. Moshkovich, Y. Gofer, D. Aurbach, Investigation of the Electrochemical Windows of Aprotic Alkali Metal (Li, Na, K) Salt Solutions, J. Electrochem. Soc. 148 (2001) 7282–7289.
[29] Z. Jian, W. Luo, X. Ji, Carbon Electrodes for K-Ion Batteries, J. Am. Chem. Soc. 137 (2015) 11566–11569.
[30] W. Zhang, Y. Liu, Z. Guo, Approaching high-performance potassium-ion batteries via advanced design strategies and engineering, Sci. Adv. 5 (2019) eaav7412.
[31] S. Dhir, et al., Outlook on K-Ion Batteries, Chem 6 (2020) 2442–2460.
[32] P. Peljo, H.H. Girault, Electrochemical potential window of battery electrolytes: the HOMO–LUMO misconception, Energy Environ. Sci. 11 (2018) 2306–2309.
[33] H. Wang, D. Zhai, F. Kang, Solid electrolyte interphase (SEI) in potassium ion batteries, Energy Environ. Sci. 13 (2020) 4583–4608.
[34] J.B. Goodenough, Y. Kim, Challenges for Rechargeable Li Batteries, Chem. Mater. 22 (2010) 587–603.
[35] S.J. An, et al., The state of understanding of the lithium-ion-battery graphite solid electrolyte interphase (SEI) and its relationship to formation cycling, Carbon 105 (2016) 52–76.
[36] Z. Li, et al., Defective Hard Carbon Anode for Na-Ion Batteries, Chem. Mater. 30 (2018) 4536–4542.
[37] G. He, L.F. Nazar, Crystallite Size Control of Prussian White Analogues for Nonaqueous Potassium-Ion Batteries, ACS Energy Lett. 2 (2017) 1122–1127.
[38] J.M. Vicent-Luna, et al., Quantum and Classical Molecular Dynamics of Ionic Liquid Electrolytes for Na/Li-based Batteries: Molecular Origins of the Conductivity Behavior, ChemPhysChem 17 (2016) 2473–2481.
[39] T. Famprikis, et al., Fundamentals of inorganic solid-state electrolytes for batteries, Nat. Mater. 18 (2019) 1278–1291.
[40] T. Hosaka, et al., Highly concentrated electrolyte solutions for 4 V class potassium-ion batteries, Chem. Commun. 54 (2018) 8387–8390.
[41] E. Cho, et al., Corrosion/passivation of aluminum current collector in bis(fluorosulfonyl)imide-based ionic liquid for lithium-ion batteries, Electrochem. Commun. 22 (2012) 1–3.
[42] Y. Yamada, et al., Corrosion Prevention Mechanism of Aluminum Metal in Superconcentrated Electrolytes, ChemElectroChem 2 (2015) 1687–1694.
[43] N. Xiao, W.D. McCulloch, Y. Wu, Reversible Dendrite-Free Potassium Plating and Stripping Electrochemistry for Potassium Secondary Batteries, J. Am. Chem. Soc. 139 (2017) 9475–9478.
[44] T. Yamamoto, et al., Physicochemical and Electrochemical Properties of $K[N(SO_2F)_2]$–[N-Methyl-N-propylpyrrolidinium][$N(SO_2F)_2$] Ionic Liquids for Potassium-Ion Batteries, J. Phys. Chem. C 121 (2017) 18450–18458.
[45] H. Gao, et al., A High-Energy-Density Potassium Battery with a Polymer-Gel Electrolyte and a Polyaniline Cathode, Angew. Chem., Int. Ed. 57 (2018) 5449–5453.
[46] S. Liu, et al., An intrinsically non-flammable electrolyte for high performance potassium batteries, Angew. Chem., Int. Ed. 59 (2020) 3638–3644.
[47] X. Bie, et al., A novel K-ion battery: hexacyanoferrate(ii)/graphite cell, J. Mater. Chem. A 5 (2017) 4325–4330.
[48] J. Liao, et al., A potassium-rich iron hexacyanoferrate/dipotassium terephthalate@carbon nanotube composite used for K-ion full-cells with an optimized electrolyte, J. Mater. Chem. A 5 (2017) 19017–19024.
[49] Q. Zhang, et al., Boosting the Potassium Storage Performance of Alloy-Based Anode Materials via Electrolyte Salt Chemistry, Adv. Energy Mater. 8 (2018) 1703288.
[50] W. Zhang, et al., Unraveling the effect of salt chemistry on long-durability high-phosphorus-concentration anode for potassium ion batteries, Nano Energy 53 (2018) 967–974.
[51] Y. Domi, et al., Potassiation and Depotassioation Properties of Sn_4P_3 Electrode in an Ionic-Liquid Electrolyte, Electrochemistry 87 (2019) 333–335.
[52] W. Zhang, et al., Understanding High-Energy-Density Sn_4P_3 Anodes for Potassium-Ion Batteries, Joule 2 (2018) 1534–1547.
[53] H. Wang, et al., Electrolyte Chemistry Enables Simultaneous Stabilization of Potassium Metal and Alloying Anode for Potassium-Ion Batteries, Angew. Chem., Int. Ed. 58 (2019) 16451–16455.
[54] L. Deng, et al., Influence of KPF_6 and KFSI on the Performance of Anode Materials for Potassium-Ion Batteries: A Case Study of MoS_2, ACS Appl. Mater. Interfaces 11 (2019) 22449–22456.
[55] J. Xie, et al., A Robust Solid Electrolyte Interphase Layer Augments the Ion Storage Capacity of Bimetallic-Sulfide-Containing Potassium-Ion Batteries, Angew. Chem., Int. Ed. 58 (2019) 14740–14747.
[56] J. Ge, et al., $MoSe_2$/N-Doped Carbon as Anodes for Potassium-Ion Batteries, Adv. Energy Mater. 8 (2018) 1801477.
[57] H. Wang, et al., A Depth-Profiling Study on the Solid Electrolyte Interface: Bis(fluorosulfuryl)imide Anion toward Improved K^+ Storage, ACS Appl. Energy Mater. 2 (2019) 7942–7951.
[58] T. Hosaka, et al., Development of KPF_6/KFSA Binary-Salt Solutions for Long-Life and High-Voltage K-Ion Batteries, ACS Appl. Mater. Interfaces 12 (2020) 34873–34881.
[59] K. Chihara, et al., $KVPO_4F$ and $KVOPO_4$ toward 4 volt-class potassium-ion batteries, Chem. Commun. 53 (2017) 5208–5211.
[60] J. Zhao, et al., Electrochemical Intercalation of Potassium into Graphite, Adv. Funct. Mater. 26 (2016) 8103–8110.
[61] A. Ponrouch, et al., In search of an optimized electrolyte for Na-ion batteries, Energy Environ. Sci. 5 (2012) 8572–8583.
[62] A. Ponrouch, et al., Towards high energy density sodium ion batteries through electrolyte optimization, Energy Environ. Sci. 6 (2013) 2361–2369.
[63] L. Deng, et al., A Nonflammable Electrolyte Enabled High Performance $K_{0.5}MnO_2$ Cathode for Low-Cost Potassium-Ion Batteries, ACS Energy Lett. 5 (2020) 1916–1922.
[64] V.A. Nikitina, et al., Effect of the electrode/electrolyte interface structure on the potassium-ion diffusional and charge transfer rates: towards a high voltage potassium-ion battery, Electrochim. Acta 258 (2017) 814–824.
[65] L. Wang, et al., Graphite as a potassium ion battery anode in carbonate-based electrolyte and ether-based electrolyte, J. Power Sources 409 (2019) 24–30.
[66] B. Li, et al., Electrolyte-Regulated Solid-Electrolyte Interphase Enables Long Cycle Life Performance in Organic Cathodes for Potassium-Ion Batteries, Adv. Funct. Mater. 29 (2018) 1807137.
[67] K. Lei, et al., High K-storage performance based on the synergy of dipotassium terephthalate and ether-based electrolytes, Energy Environ. Sci. 10 (2017) 552–557.

[68] Z. Jian, et al., Poly(anthraquinonyl sulfide) cathode for potassium-ion batteries, Electrochem. Commun. 71 (2016) 5–8.
[69] L. Zhou, et al., Electrolyte Engineering Enables High Stability and Capacity Alloying Anodes for Sodium and Potassium Ion Batteries, ACS Energy Lett. 5 (2020) 766–776.
[70] Z. Wang, et al., A nanosized SnSb alloy confined in N-doped 3D porous carbon coupled with ether-based electrolytes toward high-performance potassium-ion batteries, J. Mater. Chem. A 7 (2019) 14309–14318.
[71] L. Wang, et al., TiS_2 as a high performance potassium ion battery cathode in ether-based electrolyte, Energy Storage Mater. 12 (2018) 216–222.
[72] Y. Lei, et al., Exploring Stability of Nonaqueous Electrolytes for Potassium-Ion Batteries, ACS Appl. Energy Mater. 1 (2018) 1828–1833.
[73] L. Li, et al., Understanding High-Rate K^+-Solvent Co-Intercalation in Natural Graphite for Potassium-Ion Batteries, Angew. Chem., Int. Ed. 59 (2020) 12917–12924.
[74] S. Komaba, et al., Fluorinated Ethylene Carbonate as Electrolyte Additive for Rechargeable Na Batteries, ACS Appl. Mater. Interfaces 3 (2011) 4165–4168.
[75] A.M. Haregewoin, A.S. Wotango, B.-J. Hwang, Electrolyte additives for lithium ion battery electrodes: progress and perspectives, Energy Environ. Sci. 9 (2016) 1955–1988.
[76] S. Mai, et al., Tris(trimethylsilyl)phosphite as electrolyte additive for high voltage layered lithium nickel cobalt manganese oxide cathode of lithium ion battery, Electrochim. Acta 147 (2014) 565–571.
[77] H. Zhang, et al., Recent progresses on electrolytes of fluorosulfonimide anions for improving the performances of rechargeable Li and Li-ion battery, J. Fluorine Chem. 174 (2015) 49–61.
[78] X. Zuo, et al., Effect of diphenyl disulfide as an additive on the electrochemical performance of $Li_{1.2}Mn_{0.54}Ni_{0.13}Co_{0.13}O_2$/graphite batteries at elevated temperature, Electrochim. Acta 245 (2017) 705–714.
[79] G.G. Eshetu, et al., Electrolyte Additives for Room-Temperature, Sodium-Based, Rechargeable Batteries, Chem. Asian J. 13 (2018) 2770–2780.
[80] T. Hosaka, et al., Potassium Metal as Reliable Reference Electrodes of Nonaqueous Potassium Cells, J. Phys. Chem. Lett. 10 (2019) 3296–3300.
[81] H. Yang, et al., Potassium Difluorophosphate as an Electrolyte Additive for Potassium-Ion Batteries, ACS Appl. Mater. Interfaces 12 (2020) 36168–36176.
[82] G. Liu, et al., Additives Engineered Nonflammable Electrolyte for Safer Potassium Ion Batteries, Adv. Funct. Mater. 30 (2020) 2001934.
[83] Y. Yamada, et al., Advances and issues in developing salt-concentrated battery electrolytes, Nat. Energy 4 (2019) 269–280.
[84] Y. Yamada, A. Yamada, Review-Superconcentrated Electrolytes for Lithium Batteries, J. Electrochem. Soc. 162 (2015) A2406–A2423.
[85] Y. Yamada, A. Yamada, Superconcentrated Electrolytes to Create New Interfacial Chemistry in Non-aqueous and Aqueous Rechargeable Batteries, Chem. Lett. 46 (2017) 1056–1064.
[86] F. Chen, P. Howlett, M. Forsyth, Na-Ion Solvation and High Transference Number in Superconcentrated Ionic Liquid Electrolytes: A Theoretical Approach, J. Phys. Chem. C 122 (2018) 105–114.
[87] K.V. Kravchyk, et al., High-energy-density dual-ion battery for stationary storage of electricity using concentrated potassium fluorosulfonylimide, Nat. Commun. 9 (2018) 4469.
[88] K. Lei, et al., Dual Interphase Layers in Situ Formed on a Manganese-Based Oxide Cathode Enable Stable Potassium Storage, Chem 5 (2019) 3220–3231.
[89] L. Qin, et al., Localized High-Concentration Electrolytes Boost Potassium Storage in High-Loading Graphite, Adv. Energy Mater. 9 (2019) 1902618.
[90] W. Lu, et al., Concentrated electrolytes unlock the full energy potential of potassium-sulfur battery chemistry, Energy Storage Mater. 18 (2019) 470–475.
[91] J. Zheng, et al., Extremely stable antimony–carbon composite anodes for potassium-ion batteries, Energy Environ. Sci. 12 (2019) 615–623.
[92] L. Fan, et al., Ultrastable Potassium Storage Performance Realized by Highly Effective Solid Electrolyte Interphase Layer, Small 14 (2018) 1801806.
[93] C.D. Wessells, et al., Nickel Hexacyanoferrate Nanoparticle Electrodes for Aqueous Sodium and Potassium Ion Batteries, Nano Lett. 11 (2011) 5421–5425.
[94] R. Li, et al., Carbon-Stabilized High-Capacity Ferroferric Oxide Nanorod Array for Flexible Solid-State Alkaline Battery–Supercapacitor Hybrid Device with High Environmental Suitability, Adv. Funct. Mater. 25 (2015) 5384–5394.
[95] D. Su, et al., High-capacity aqueous potassium-ion batteries for large-scale energy storage, Adv. Mater. 29 (2017) 1604007.
[96] Q. Zheng, et al., Sodium- and Potassium-Hydrate Melts Containing Asymmetric Imide Anions for High-Voltage Aqueous Batteries, Angew. Chem., Int. Ed. 58 (2019) 14202–14207.
[97] D.P. Leonard, et al., Water-in-Salt Electrolyte for Potassium-Ion Batteries, ACS Energy Lett. 3 (2018) 373–374.
[98] L. Jiang, et al., Building aqueous K-ion batteries for energy storage, Nat. Energy 4 (2019) 495–503.
[99] Z. Liu, et al., Voltage issue of aqueous rechargeable metal-ion batteries, Chem. Soc. Rev. 49 (2020) 180–232.
[100] T. Yamamoto, T. Nohira, Tin negative electrodes using an FSA-based ionic liquid electrolyte: improved performance of potassium secondary batteries, Chem. Commun. 56 (2020) 2538–2541.
[101] M. Kato, et al., Organic positive-electrode material utilizing both an anion and cation: a benzoquinone-tetrathiafulvalene triad molecule, Q-TTF-Q, for rechargeable Li, Na, and K batteries, New J. Chem. 43 (2019) 1626–1631.
[102] M. Fiore, et al., Paving the Way toward Highly Efficient, High-Energy Potassium-Ion Batteries with Ionic Liquid Electrolytes, Chem. Mater. 32 (2020) 7653–7661.
[103] K. Yoshii, et al., Sulfonylamide-Based Ionic Liquids for High-Voltage Potassium-Ion Batteries with Honeycomb Layered Cathode Oxides, ChemElectroChem 6 (2019) 3901–3910.
[104] T. Masese, et al., A high voltage honeycomb layered cathode framework for rechargeable potassium-ion battery: P2-type $K_{2/3}Ni_{1/3}Co_{1/3}Te_{1/3}O_2$, Chem. Commun. 55 (2019) 985–988.
[105] T. Masese, et al., Rechargeable potassium-ion batteries with honeycomb-layered tellurates as high voltage cathodes and fast potassium-ion conductors, Nat. Commun. 9 (2018) 3823.
[106] M. Arnaiz, et al., Aprotic and protic ionic liquids combined with olive pits derived hard carbon for potassium-ion batteries, J. Electrochem. Soc. 166 (2019) A3504–A3510.
[107] K. Beltrop, et al., Alternative electrochemical energy storage: potassium-based dual-graphite batteries, Energy Environ. Sci. 10 (2017) 2090–2094.
[108] H. Yamamoto, et al., Potassium Single Cation Ionic Liquid Electrolyte for Potassium-Ion Batteries, J. Phys. Chem. B 124 (2020) 6341–6347.
[109] P. Liu, et al., Dendrite-Free Potassium Metal Anodes in a Carbonate Electrolyte, Adv. Mater. 32 (2020) 1906735.
[110] B. Ji, et al., A Dual-Carbon Battery Based on Potassium-Ion Electrolyte, Adv. Energy Mater. 7 (2017) 1700920.
[111] A.P. Cohn, et al., Durable potassium ion battery electrodes from high-rate cointercalation into graphitic carbons, J. Mater. Chem. A 4 (2016) 14954–14959.
[112] Y. Lei, et al., Unveiling the influence of electrode/electrolyte interface on the capacity fading for typical graphite-based potassium-ion batteries, Energy Storage Mater. 24 (2020) 319–328.
[113] K. Lei, et al., A Porous Network of Bismuth Used as the Anode Material for High-Energy-Density Potassium-Ion Batteries, Angew. Chem., Int. Ed. 57 (2018) 4687–4691.
[114] L. Fan, et al., Graphite Anode for a Potassium-Ion Battery with Unprecedented Performance, Angew. Chem., Int. Ed. 58 (2019) 10500–10505.
[115] X. Niu, et al., Salt-concentrated electrolytes for graphite anode in potassium ion battery, Solid State Ionics 341 (2019) 115050.
[116] R. Zhang, et al., Concentrated electrolytes stabilize bismuth–potassium batteries, Chem. Sci. 9 (2018) 6193–6198.
[117] L. Fan, et al., An Ultrafast and Highly Stable Potassium–Organic Battery, Adv. Mater. 30 (2018) 1805486.
[118] J. Wang, et al., In Situ Alloying Strategy for Exceptional Potassium Ion Batteries, ACS Nano 13 (2019) 3703–3713.
[119] X. Liu, et al., Highly Concentrated KTFSI: Glyme Electrolytes for K/Bilayered-V_2O_5 Batteries, Batteries Supercaps 3 (2020) 261–267.
[120] J. Li, et al., K-Ion Storage Enhancement in Sb_2O_3/Reduced Graphene Oxide Using Ether-Based Electrolyte, Adv. Energy Mater. 10 (2020) 1903455.
[121] Q. Peng, et al., Boosting Potassium Storage Performance of the Cu_2S Anode via Morphology Engineering and Electrolyte Chemistry, ACS Nano 14 (2020) 6024–6033.
[122] N.S. Katorova, et al., Effect of Concentrated Diglyme-Based Electrolytes on the Electrochemical Performance of Potassium-Ion Batteries, ACS Appl. Energy Mater. 2 (2019) 6051–6059.
[123] Z. Tong, et al., Tailored Redox Kinetics, Electronic Structures and Electrode/Electrolyte Interfaces for Fast and High Energy-Density Potassium-Organic Battery, Adv. Funct. Mater. 30 (2020) 1907656.
[124] P. Münster, et al., Enabling High Performance Potassium-Based Dual-Graphite Battery Cells by Highly Concentrated Electrolytes, Batteries Supercaps 2 (2019) 992–1006.
[125] X. Li, X. Ou, Y. Tang, 6.0 V High-Voltage and Concentrated Electrolyte toward High Energy Density K-Based Dual-Graphite Battery, Adv. Energy Mater. 10 (2020) 2002567.
[126] Y. Li, et al., Dual-phase nanostructuring of layered metal oxides for high-performance aqueous rechargeable potassium ion microbatteries, Nat. Commun. 10 (2019) 4292.
[127] J. Han, et al., Gelified acetate-based water-in-salt electrolyte stabilizing hexacyanoferrate cathode for aqueous potassium-ion batteries, Energy Storage Mater. 30 (2020) 196–205.
[128] A. Gros, S. Sakong, Modelling the electric double layer at electrode/electrolyte interfaces, Curr. Opin. Electrochem. 14 (2019) 1–6.
[129] L. Zhang, X.S. Zhao, Carbon-based materials as supercapacitor electrodes, Chem. Soc. Rev. 38 (2009) 2520–2531.
[130] C. Yan, et al., Toward Critical Electrode/Electrolyte Interfaces in Rechargeable Batteries, Adv. Funct. Mater. 30 (2020) 1909887.
[131] J. Zhang, et al., Model-Based Design of Stable Electrolytes for Potassium Ion Batteries, ACS Energy Lett. 5 (2020) 3124–3131.
[132] J. Huang, et al., Bismuth Microparticles as Advanced Anodes for Potassium-Ion Battery, Adv. Energy Mater. 8 (2018) 1703496.
[133] Y. Gu, et al., Designable ultra-smooth ultra-thin solid-electrolyte interphases of three alkali metal anodes, Nat. Commun. 9 (2018) 1339.
[134] H. Wang, et al., Potassium Metal Batteries: Artificial Solid-Electrolyte Interphase Enabled High-Capacity and Stable Cycling Potassium Metal Batteries, Adv. Energy Mater. 9 (2019) 1970168.
[135] J. Hui, et al., Achieving Fast and Efficient K^+ Intercalation on Ultrathin Graphene Electrodes Modified by a Li^+ Based Solid-Electrolyte Interphase, J. Am. Chem. Soc. 140 (2018) 13599–13603.